

Sbottoms of natural NMSSM at the LHC

Jyotiranjana Beuria^{a,b} Arindam Chatterjee^c Asesh Krishna Datta^a

^a*Harish-Chandra Research Institute, Allahabad 211019, India*

^b*Regional Centre for Accelerator-based Particle Physics
Harish-Chandra Research Institute, Allahabad 211019, India*

^c*Physics and Applied Mathematics Unit, Indian Statistical Institute,
203 B.T. Road, Kolkata 700108, India*

E-mail: jyotiranjana@hri.res.in, arin_t@isical.ac.in, asesh@hri.res.in

ABSTRACT: Search for the bottom squarks (sbottoms) at the Large Hadron Collider (LHC) has recently assumed a heightened focus in the hunt for Supersymmetry (SUSY). The popular framework of the Next-to-Minimal Supersymmetric Standard Model (NMSSM) could conceive a naturally light sbottom which can easily be consistent with available constraints from the experiments at the LHC. Phenomenology of such sbottoms could in principle be as striking as that for a light top squark (stop) thanks to a rather nontrivial neutralino sector (with appreciable mixing among the neutral higgsinos and the singlino) that the scenario gives rise to. Nonetheless, finding such sbottoms would require a moderately large volume of data ($\sim 300 \text{ fb}^{-1}$) at the 13 TeV run of the LHC. A multi-channel analysis establishing a generic depletion of events in the usual $2b\text{-jets} + \cancel{E}_T$ final state while registering, in conjunction, characteristically significant rates in various multi-lepton final states accompanied by $b\text{-jets}$ might point not only to the presence of light sbottom(s) but could also shed crucial light on their compositions and the (singlino) nature of the lightest SUSY particle (LSP).

KEYWORDS: Hadronic Colliders, Beyond Standard Model, Supersymmetry Phenomenology

Contents

1	Introduction	1
2	The theoretical setup	4
2.1	The sbottom and the stop sectors	4
2.2	The Higgs sector	5
2.3	The neutralinos and the charginos	6
2.4	Relevant interactions	7
3	Sbottoms at the LHC Run-I	8
3.1	The case with a light $\tilde{b}_1 \equiv \tilde{b}_L$	9
3.2	The case with a light $\tilde{b}_1 \equiv \tilde{b}_R$	12
3.3	The case with $m_{\tilde{b}_1} < m_t + m_{\tilde{\chi}_1^-}$	12
3.4	Effect of mixing in the sbottom sector	13
4	Benchmark scenarios and the 13 TeV LHC	15
4.1	Benchmark scenarios	15
4.2	Sbottoms at the LHC-13	16
4.3	Simulation setup and selection of final states	18
4.4	Results and discussion	19
5	Conclusions	24

1 Introduction

It is well known that squarks from the third generation, in particular, the top squarks (stops), are capable of providing a ‘natural’ supersymmetric (SUSY) solution to the notorious hierarchy problem that cripples the scalar (Higgs) sector of the Standard Model (SM) if they are relatively light ($\lesssim 1$ TeV). Over the years, this has motivated the search for sub-TeV stops at the collider experiments and recently, at the Large Hadron Collider (LHC), hunt for them has expectedly taken the centre stage. The latest analyses of the data from the 7 TeV and 8 TeV runs of the LHC (collectively termed as the LHC Run-I in this work) [1, 2] have resulted in stringent lower bounds on the stop mass, under varied assumptions over how it decays. The most conservative of these bounds says that the lighter stop should be heavier than ~ 700 GeV [2]. A reasonably performing 13 TeV run of the LHC (LHC-13), currently underway, could quickly and substantially improve on these bounds thus pushing them around a TeV.

On the other hand, over the past few years, there has been a growing interest in the phenomenology of the bottom squarks (sbottoms) [3–15], the other squarks from the third

generation. Also, in recent years, implications of the LHC results for the squarks from the third generation in a ‘natural’ SUSY setup [16] are studied intensively [17–20]. This has a solid motivation. Although the sbottom sector is not broadly as instrumental as the stop sector for rendering SUSY ‘natural’ (due to its relatively much smaller coupling to the Higgs boson), sbottoms are rather close cousins of the stops. In particular, the left-handed (L-type) stop and the sbottom (\tilde{t}_L and \tilde{b}_L) live in the same weak doublet and enjoy an approximate custodial symmetry [5]. Quantitatively, its breaking is restricted by electroweak precision data via the well-known Peskin-Takeuchi STU (oblique) parameters [21]. On the theoretical side, the soft masses for these L-type states are $SU(2)_L$ -invariant and hence equal. However, a modest splitting occurs due to $SU(2)_L$ -breaking D -term (which is a function of $\tan\beta = \frac{v_u}{v_d}$, the ratio of vacuum expectation values of the neutral components of the two Higgs doublets) and because of the presence of an F -term which goes as the corresponding quark (top or bottom) mass. This implies that at least one squark state from each flavor (which are dominantly L-type) would have comparable masses. Only a rather large mixing in the stop sector could obscure this phenomenon under certain circumstances. On the other hand, the masses of the right-handed (R-type) stop and the sbottom ($m_{\tilde{t}_R}$ and $m_{\tilde{b}_R}$) are neither related by any symmetry nor do they bear any relation to their corresponding L-type partners. Thus, they can assume any value allowed by applicable searches at the colliders. Hence if the lighter stop is accessible to the LHC experiments and happens to be mostly L-type, the same should be true for a sbottom which is also dominantly L-type. This substantiates the increased interest in the search for sbottoms at the LHC. On the other hand, a relatively light R-type sbottom can be present while the other sbottom and both stops are relatively heavy¹.

It is somewhat interesting to note that various possible decay modes of the sbottom have recently been explored rigorously for the first time by the experimental searches at the LHC [1, 2, 26–28]. These result in lower bounds on $m_{\tilde{b}_1}$ roughly ranging between 500-750 GeV. Subsequently, these findings are exploited by the phenomenological works providing further insight [8, 15]. However, these studies are heavily based on the popular framework of the Minimal SUSY extension of the Standard Model (MSSM). In the present work, we look into the phenomenology of possibly light sbottom(s) in the framework of the next-to-MSSM (NMSSM) [29], a scenario which has assumed a renewed relevance in view of the recent Higgs results from the LHC.

Issues with sbottom search vis-a-vis stop search have already been discussed in the literature [30]. For example, search for stop squarks may suffer from large background from the SM top quark production when the decay $\tilde{t}_1 \rightarrow t\chi_1^0$ is dominant. This is not the case with sbottom search in one of its preferred decay modes, i.e., $\tilde{b}_1 \rightarrow b\chi_1^0$. On the other hand, depending on how they decay, stop and sbottom could lead to the same final states thus making it somewhat difficult to extract unambiguous information. Combining analyses for the sbottom and stop to find an optimal sensitivity to a given region in the parameter space

¹ It may, however, be noted that presence of relatively heavy stops (and/or a gluino) may not be an immediate threat to naturalness as revealed by certain recent parameterizations in the MSSM context that refer only to weak scale values of the parameters as long as $|\mu|$ ($|\mu_{eff}|$, in NMSSM) is small enough which is essential to the scenario presented in this work [22–25].

parameter has recently been advocated in reference [15].

The popular framework of the NMSSM offers new possibilities in this context. First, the scope of having a richer electroweak gaugino sector (a mixture of a singlino, higgsinos and gauginos) with relatively light states could lead to interesting phenomenology of the stop and the sbottom through their decays to these states. Secondly, the NMSSM can easily accommodate relatively light stops without being in conflict with the observations in the Higgs sector [31]. If such a light stop happens to be dominantly L-type in nature, there is going to be an L-type sbottom close-by in mass to the light stop. These two issues render the NMSSM to be a ‘natural’ setup to study the sbottom sector. Interesting aspects of such a scenario and their phenomenology have recently been pointed out mainly in the context of (or in terms of) relatively light stops accompanied by a singlino-like neutralino LSP while the lighter chargino and a pair of immediately heavier neutralinos are higgsino-like [31, 32].

In the present work, we focus on relatively light sbottom(s) with varied compositions whose phenomenology might turn out to be more tractable than that of the stops. This is since the extent of mixing that could be present in the sbottom sector is much smaller than that possible in the stop sector. We adopt a setup inspired by naturalness and hence with low values of the effective μ parameter (μ_{eff}) [33]. This exploits the original scope in the NMSSM to dynamically generate such a low value of μ_{eff} via a suitable choice of the vacuum expectation value (*vev*) v_S of the singlet scalar field, a defining feature of such a scenario. As we shall see, this opens up further possibilities of not only having a singlino-like lightest SUSY particle (LSP) but also nontrivial mixings among the singlino and the higgsinos. Impact of the singlino on the NMSSM phenomenology under specific circumstances have been discussed in the literature [34–39]. Here, we investigate how the mixed singlino-higgsino LSP would alter the decay pattern of the sbottom in characteristic ways. In particular, for a mostly L-type sbottom, its decay to higgsino-like lighter chargino is driven by the top Yukawa coupling and hence could dominate, in particular, at low $\tan\beta$. In contrast, decays of a dominantly R-type light sbottom to lighter higgsinos-like states (both chargino and neutralinos) are all governed by the bottom Yukawa coupling and thus, could become comparable.

Light stops when accompanied by a modest value of μ_{eff} could further ensure a lower fine-tuning in the setup. These together add another perspective to the current issue. A stop lighter than what is achievable in the MSSM (being compatible with the observed Higgs mass) can be obtained for larger values of the λ parameter in the NMSSM. Note that λ couples the singlet state to the doublet Higgs states in the NMSSM superpotential. However, given the relationship $\mu_{\text{eff}} = \lambda v_S$, a smaller value of μ_{eff} would then require a relatively small v_S . On the other hand, avoiding appearance of Landau pole below the unification (GUT) scale restricts κ to smaller values when λ is large. As we will see later, a small μ_{eff} combined with smaller κ but a large λ , could induce a significant mixing among the higgsinos and the singlino before reaching a point when the LSP becomes singlino-like with $m_{LSP} \approx m_{\tilde{\chi}} = 2\kappa v_S$.

The paper is organized as follows. In section 2 we outline the theoretical setup for the Z_3 -invariant NMSSM by briefly discussing the sbottom (stop) sector, the Higgs sector, the sectors involving the charginos and the neutralinos and the relevant interactions among these states which are germane to the present work. In section 3 we look into the status of sbottom search

at the end of the LHC Run-I when interpreted in the NMSSM framework. We take a critical look into the cases with sbottoms(s) having varied compositions and their phenomenological ramifications. Section 4 is devoted to identifying a few benchmark scenarios based on the findings of section 3 followed by the presentation of their detailed simulation at the 13 TeV run of the LHC. In section 5 we conclude.

2 The theoretical setup

The present work relies on a popular NMSSM framework known as the Z_3 -invariant NMSSM. The superpotential is given by

$$\mathcal{W} = \mathcal{W}_{\mathcal{MSSM}}|_{\mu=0} + \lambda \hat{S} \hat{H}_u \cdot \hat{H}_d + \frac{\kappa}{3} \hat{S}^3. \quad (2.1)$$

Here, $\mathcal{W}_{\mathcal{MSSM}}$ is the MSSM superpotential, \hat{H}_u and \hat{H}_d stand for the doublet Higgs superfields while the gauge singlet superfield, characterizing the NMSSM, is denoted by \hat{S} . The corresponding soft-supersymmetry breaking terms are given by

$$-\mathcal{L}_{\text{soft}} = -\mathcal{L}_{\text{soft}}^{\text{MSSM}}|_{B\mu=0} + m_S^2 |S|^2 + \lambda A_\lambda S H_u \cdot H_d + \frac{1}{3} \kappa A_\kappa S^3 + \text{h.c.} + \dots \quad (2.2)$$

where $\mathcal{L}_{\text{soft}}^{\text{MSSM}}$ represents the soft SUSY-breaking terms in the MSSM, A_λ and A_κ are the new trilinear soft SUSY-breaking terms (with dimensions of mass) that are present in the NMSSM while m_S^2 is the soft SUSY-breaking mass term for the singlet scalar S of the NMSSM.

In the rest of this section we briefly discuss the salient features of the sbottom and the stop sectors, the Higgs sector and the sector involving the neutralinos and the charginos (the electroweakinos). The stop and the Higgs sector play crucial roles in motivating and defining the overall scenario that we work in while, in our ‘simplified’ approach, except for some involved situations, these are only the sbottoms and the electroweakinos that directly shape up the interesting phenomenology pertaining to the sbottoms in the NMSSM.

2.1 The sbottom and the stop sectors

At the tree level, the mass-squared matrices for the sbottom and the stop squarks in the NMSSM are similar to the corresponding ones in the MSSM with μ in the off-diagonal terms being replaced by μ_{eff} ($= \lambda v_S$). These are given, at the tree level, by the following 2×2 matrices in the bases $\{m_{\tilde{b}_L}, m_{\tilde{b}_R}\}$ and $\{m_{\tilde{t}_L}, m_{\tilde{t}_R}\}$, respectively;

$$\mathcal{M}_{\tilde{b}} = \begin{pmatrix} m_{\tilde{Q}_3}^2 + y_b^2 v_d^2 + (v_u^2 - v_d^2) \left(\frac{g_1^2}{12} + \frac{g_2^2}{4} \right) & y_b (A_b v_d - \mu_{\text{eff}} v_u) \\ y_b (A_b v_d - \mu_{\text{eff}} v_u) & m_{\tilde{D}_3}^2 + y_b^2 v_d^2 + (v_u^2 - v_d^2) \frac{g_1^2}{6} \end{pmatrix} \quad (2.3)$$

and

$$\mathcal{M}_{\tilde{t}} = \begin{pmatrix} m_{\tilde{Q}_3}^2 + y_t^2 v_u^2 + (v_u^2 - v_d^2) \left(\frac{g_1^2}{12} - \frac{g_2^2}{4} \right) & y_t (A_t v_u - \mu_{\text{eff}} v_d) \\ y_t (A_t v_u - \mu_{\text{eff}} v_d) & m_{\tilde{U}_3}^2 + y_t^2 v_u^2 - (v_u^2 - v_d^2) \frac{g_1^2}{3} \end{pmatrix}. \quad (2.4)$$

In the above two equations $m_{\tilde{Q}_3}$, $m_{\tilde{D}_3}$ and $m_{\tilde{U}_3}$ denote the soft SUSY breaking mass terms for the $SU(2)$ doublet (L-type) and the singlet (R-type) sbottom and stop squarks, respectively. $y_{b,t}$ are the respective Yukawa couplings while $A_{b,t}$ -s are the respective trilinear soft SUSY breaking terms. v_d and v_u stand for the vev 's of the CP-even down- and up-type neutral Higgs bosons, H_d^0 and H_u^0 , respectively. g_1 and g_2 denote the gauge couplings for the $U(1)_Y$ and $SU(2)_L$ gauge groups, respectively. We also define a generic rotation matrix $\mathcal{R}_{\tilde{f}}$ that diagonalizes the sbottom and stop mass matrices as follows:

$$\mathcal{R}_{\tilde{f}} = \begin{pmatrix} \cos \theta_{\tilde{f}} & \sin \theta_{\tilde{f}} \\ -\sin \theta_{\tilde{f}} & \cos \theta_{\tilde{f}} \end{pmatrix} \quad (2.5)$$

where \tilde{f} stands for \tilde{b} or \tilde{t} , respectively and $\theta_{\tilde{f}}$, at the tree level, is still given by its standard MSSM expression

$$\sin 2\theta_{\tilde{f}} = \frac{2m_f X_f}{m_{\tilde{f}_2}^2 - m_{\tilde{f}_1}^2} \quad , \quad X_f = A_{\tilde{f}} - \mu_{\text{eff}} r \quad , \quad (2.6)$$

where $r = \tan \beta (\cot \beta)$ for the sbottom (stop) sector, m_f is the corresponding fermion mass while $m_{\tilde{f}_{1,2}}$ stand for the masses of the lighter and the heavier sbottom/stop eigenstates, respectively. In this convention, $\theta_{\tilde{f}} = 0(\frac{\pi}{2})$ corresponds to the unmixed L-type (R-type) state to be the lightest mass eigenstate.

Clearly, if $m_{\tilde{Q}_3}$ is relatively small, one could expect a light sbottom along with a light stop close-by in mass, both of them being dominantly L-type. It could also, in general, be noted that since $y_b \ll y_t$, mixing between the L- and the R-type sbottom states can at best be modest (when compared to the stop sector). Thus, the physical sbottoms are nearly pure ‘chiral’ states and hence their phenomenology is more tractable. Nonetheless, as we will later see, even such a small mixing could, under certain circumstances, lead to very interesting phenomenology for the sbottoms.

2.2 The Higgs sector

The Higgs sector of the NMSSM also gets extended nontrivially when compared to its MSSM counterpart with the inclusion of a singlet scalar S belonging to the singlet superfield \hat{S} . On electroweak symmetry breaking, CP even components of the three neutral scalar fields, H_u , H_d and S , mix to give rise to three CP-even Higgs bosons of the NMSSM. The mass of the SM-like Higgs boson is given by [40]

$$m_h^2 = m_Z^2 \cos^2 2\beta + \lambda^2 v^2 \sin^2 2\beta + \Delta_{\text{mix}} + \Delta_{\text{rad.corr.}} \quad (2.7)$$

with $v = \sqrt{v_u^2 + v_d^2} \simeq 174 \text{ GeV}$. The first term in the right hand side of 2.7 gives the tree level squared mass of the SM-like Higgs boson in the MSSM. The term proportional to λ^2 is the NMSSM contribution at the tree level. The term Δ_{mix} originates in the so-called singlet-doublet mixing. In the limit of weak mixing, this is given by

$$\Delta_{\text{mix}} = \frac{4\lambda^2 v_S^2 v^2 (\lambda - \kappa \sin 2\beta)^2}{\tilde{m}_h^2 - m_{ss}^2} \quad (2.8)$$

with $\tilde{m}_h^2 = m_h^2 - \Delta_{\text{mix}}$ and $m_{ss}^2 = \kappa v_S(A_\kappa + 4\kappa v_S)$. The additional NMSSM contribution at the tree level could enhance the mass of the SM-like Higgs boson to a level such that to conform to the observed mass, it does not need to bank much upon the radiative corrections [31, 40]. Hence smaller values of stop masses (and/or smaller mixing in the stop sector) can be easily afforded thus rendering the framework more ‘natural’.

Although the sbottom sector could only play a subdominant role in issues pertaining to ‘naturalness’, its phenomenology, nonetheless, could significantly exploit such upshots in the NMSSM stop sector. To conform to the observed mass of the SM-like Higgs boson, a scenario with light stops in the NMSSM prefers a genuinely low $\tan\beta$ ($\lesssim 5$) [31, 41, 42]. As we will discuss in the subsequent sections, this shapes the phenomenology of the sbottoms in a novel way. It may be reiterated that a light stop which is mostly L-type is accompanied by an L-type sbottom having a close-by mass. An sbottom which is mostly R-type, however, can be light independent of the masses of the stops. As we shall see, in both cases, light sbottoms could easily escape experimental bounds in a simplified NMSSM framework that we adopt in this work.

2.3 The neutralinos and the charginos

The compositions of the neutralinos and the charginos are crucial to the phenomenology of the sbottoms (and of the stops, as well). While the structure of the chargino sector of the NMSSM (at the tree level) is identical to that of the MSSM, the neutralino sector has some essential difference. The difference arises from the presence of the fermionic component \tilde{S} corresponding to the singlet superfield \hat{S} present in the NMSSM superpotential (see equation 2.1). The singlino could mix with the higgsinos and the gauginos. As we shall see, this could lead to an LSP which has a significant singlino admixture thus affecting crucially the cascade decay patterns of the heavier SUSY particles. We assume conserved R -parity and hence a stable LSP.

The symmetric 5×5 neutralino mass matrix is given by

$$\mathcal{M}_0 = \begin{pmatrix} M_1 & 0 & -\frac{g_1 v_d}{\sqrt{2}} & \frac{g_1 v_u}{\sqrt{2}} & 0 \\ & M_2 & \frac{g_2 v_d}{\sqrt{2}} & -\frac{g_2 v_u}{\sqrt{2}} & 0 \\ & & 0 & -\mu_{\text{eff}} & -\lambda v_u \\ & & & 0 & -\lambda v_d \\ & & & & 2\kappa v_S \end{pmatrix} \quad (2.9)$$

in the basis $\psi^0 = \{\tilde{B}, \tilde{W}^0, \tilde{H}_d^0, \tilde{H}_u^0, \tilde{S}\}$ [29, 43]. In the above expression, M_1 and M_2 stand for the soft SUSY-breaking masses of the $U(1)$ (\tilde{B}) and the $SU(2)$ (\tilde{W}) gauginos, respectively. The rest of the variables appearing in equation 2.9 have already been introduced in the text. The above mass-matrix can be diagonalized by a matrix N [29, 43]:

$$N^* \mathcal{M}_0 N^\dagger = \text{diag}(\chi_1^0, \chi_2^0, \chi_3^0, \chi_4^0, \chi_5^0) \quad (2.10)$$

such that the five neutralino mass-eigenstates (in order of increasing mass as ‘ i ’ varies from 1 to 5, in our present study) can be written in a compact form in terms of the five weak

eigenstates (ψ_j , with $j = 1, \dots, 5$) as

$$\chi_i^0 = N_{ij} \psi_j^0 \quad (2.11)$$

As can be gleaned from the entries of the mass matrix, the singlino state mixes with the gaugino states only via the higgsino sector. Hence these mixings are rather suppressed. In contrast, the singlino-higgsino mixing is direct and could be appreciable depending upon the relative values of μ_{eff} , $2\kappa v_S (= m_{\tilde{\chi}})$ and the value of λ . Thus, in a setup where μ_{eff} and $2\kappa v_S$ are small but of comparable magnitudes, the neutralino sector becomes rather involved with the presence of low-lying neutralino states (including the LSP) having widely varying singlino admixtures. This can alter the phenomenology of the light squarks in an essential manner, in particular, that of the light sbottoms which is the subject of the present work.

The chargino mass matrix of the NMSSM scenario under consideration, in the basis

$$\psi^+ = \begin{pmatrix} -i\tilde{W}^+ \\ \tilde{H}_u^+ \end{pmatrix}, \quad \psi^- = \begin{pmatrix} -i\tilde{W}^- \\ \tilde{H}_d^- \end{pmatrix}, \quad (2.12)$$

is given by

$$\mathcal{M}_C = \begin{pmatrix} M_2 & g_2 v_u \\ g_2 v_d & \mu_{\text{eff}} \end{pmatrix}. \quad (2.13)$$

This differs from \mathcal{M}_C of the MSSM in the entry μ_{eff} (which is μ for the MSSM). As in the MSSM, this asymmetric matrix is diagonalized by two 2×2 unitary matrices U and V :

$$U^* \mathcal{M}_C V^\dagger = \text{diag}(m_{\tilde{\chi}_1^\pm}, m_{\tilde{\chi}_2^\pm}) \quad (2.14)$$

with $m_{\tilde{\chi}_1^\pm} < m_{\tilde{\chi}_2^\pm}$.

Relevant interactions involving the sbottom, the neutralinos, the chargino and the Higgs boson are discussed in section 2.4. In the present work, we restrict ourselves in a ‘simplified’ setup where the lighter three neutralinos are typically light and are mixtures of the singlino and the higgsino states while the lighter chargino is almost purely higgsino. The heavier states from both the sectors are made to be heavy enough by choosing M_1 and M_2 to be rather large so that they mostly decouple from the phenomenology.

2.4 Relevant interactions

In the context of the present work, the important interactions are those involving the sbottoms, the neutralinos and the charginos. While we would rely on the strong production modes of the sbottoms (in pairs), the phenomenology would crucially depend not only on how the sbottoms decay to neutralinos and the charginos, but also on how these decay products cascade down to the LSP. Below we outline these interactions in brief.

Interactions of sbottom with neutralinos are of the generic form

$$b\tilde{b}_i \tilde{\chi}_n^0 : \quad g_2 \tilde{b} \left(a_{in}^{\tilde{b}} P_R + b_{in}^{\tilde{b}} P_L \right) \tilde{\chi}_n^0 \tilde{b}_i + \text{h.c.}$$

which is similar to the MSSM case except for the fact that the neutralino index ‘ n ’ now runs from 1 to 5 (see equation 2.9) [43] to include a singlino-like state. $P_{R,L}$ are the standard

projection operators given by $\frac{1\pm\gamma_5}{2}$. However, couplings of sbottoms to charginos are identical to those in the MSSM and are given by [44]

$$t\tilde{b}_i\tilde{\chi}_j^+ : g_2\bar{t}\left(l_{ij}^{\tilde{b}}P_R + k_{ij}^{\tilde{b}}P_L\right)\tilde{\chi}_j^+\tilde{b}_i + \text{h.c.} \quad .$$

In the above expressions, $a_{in}^{\tilde{b}}$, $b_{in}^{\tilde{b}}$, $l_{ij}^{\tilde{b}}$ and $k_{ij}^{\tilde{b}}$ are all as given in reference [44]. Nonetheless, for future purposes, we write down the factors $l_{ij}^{\tilde{b}}$ and $k_{ij}^{\tilde{b}}$ (that appear in the decays of sbottoms to the chargino states) explicitly as follows:

$$l_{ij}^{\tilde{b}} = -\mathcal{R}_{i1}U_{j1} + y_b\mathcal{R}_{i2}U_{j2}, \quad k_{ij}^{\tilde{b}} = y_t\mathcal{R}_{i1}V_{j2}^*$$

and $y_b = \frac{m_b}{\sqrt{2}m_W\cos\beta}$ and $y_t = \frac{m_t}{\sqrt{2}m_W\sin\beta}$.

The decays of neutralinos and the lighter chargino that involve the Higgs bosons (in particular, the light, neutral ones) and the gauge (Z and W) bosons are governed by the following interactions. The Higgs-neutralino-neutralino coupling is given by

$$\begin{aligned} H_a\chi_i^0\chi_j^0 : & \frac{\lambda}{\sqrt{2}}(S_{a1}\Pi_{ij}^{45} + S_{a2}\Pi_{ij}^{35} + S_{a3}\Pi_{ij}^{34}) - \sqrt{2}\kappa_i S_{a3}N_{i5}N_{j5} \\ & + \frac{g_1}{2}(S_{a1}\Pi_{ij}^{13} - S_{a2}\Pi_{ij}^{14}) - \frac{g_2}{2}(S_{a1}\Pi_{ij}^{23} - S_{a2}\Pi_{ij}^{24}) \end{aligned}$$

where $\Pi_{ij}^{ab} = N_{ia}N_{jb} + N_{ib}N_{ja}$ [29] and N is given by equations 2.10 and 2.11. On the other hand, the Z -neutralino-neutralino coupling is determined by the factor [45]

$$Z\chi_i^0\chi_j^0 : g_2(N_{i3}N_{j3} - N_{i4}N_{j4})$$

while W^\pm -chargino-neutralino interaction is determined by the two bilinear charges \mathcal{W}_L and \mathcal{W}_R where [45]

$$W^\pm\chi_i^\mp\chi_j^0 : \left\{ g_2\mathcal{W}_{Lij} = g_2(U_{i1}^*N_{j2} + \frac{1}{\sqrt{2}}U_{i2}^*N_{j3}), \quad g_2\mathcal{W}_{Rij} = g_2(V_{i1}^*N_{j2}^* - \frac{1}{\sqrt{2}}V_{i2}^*N_{j4}^*) \right\},$$

U and V being the unitary matrices given by equation 2.14. All through, g_1 and g_2 stand for $U(1)$ and $SU(2)$ gauge couplings, respectively.

3 Sbottoms at the LHC Run-I

As has been mentioned earlier, given that only a modest mixing between L- and R-type sbottom states is possible, broad phenomenological studies involving sbottoms can safely be carried out presuming them to be pure ‘chiral’ states. Hence in the subsequent discussions, we would systematically take up the cases of a light sbottom which is either L- or R-type. However, in the light of the discussion above, we would also demonstrate the impact of even a minuscule admixture of L-type sbottom in the lighter sbottom state which is otherwise dominantly R-type.

3.1 The case with a light $\tilde{b}_1 \equiv \tilde{b}_L$

The published bounds on the mass of $\tilde{b}_1 \equiv \tilde{b}_L$ from the LHC Run-I [1, 2] vary depending on how it decays². As indicated in the Introduction, it touches ~ 650 GeV when \tilde{b}_L decays 100% of the times into the b -LSP mode. However, in a scenario with relatively light higgsino-like neutralinos, \tilde{b}_L could decay into these states. Unlike in the MSSM, where these decays would be suppressed since these are driven by the weak bottom Yukawa coupling (which cannot compete with an analogous setup with, say, a bino/wino-like LSP neutralino), in the case of the NMSSM these would dominate. This is precisely since, in our scenario, the LSP is more like a singlino and thus its coupling to sbottom would be suppressed. Thus, in the present case, \tilde{b}_L could dominantly decay to higgsino-like neutralinos followed by the latter decaying to the singlino-like LSP. The other possibility, under such a circumstance, is that \tilde{b}_L decays to a higgsino-like chargino and a top quark. Note that once the phase space for this decay is available, this could be the dominant two-body decay mode for \tilde{b}_L since it is driven by the top Yukawa coupling. Hence, in any case, the assumption of $\text{BR}[\tilde{b}_L \rightarrow b \text{ LSP}]$ would not hold for our scenario and the mass-bound on \tilde{b}_L mentioned above is easily evaded.

It can now be noted that the published bound on the light sbottom mass touches ~ 470 GeV when the two-body decay branching ratios $\text{BR}[\tilde{b}_1 \rightarrow t\chi_1^-]$ followed by $\text{BR}[\chi_1^\mp \rightarrow W^\mp\chi_1^0]$ are both 100% [2, 28]. Such decays can give rise to same-sign dilepton (SSDL) final states (which are used to put the above bound) thanks to two sources of W -boson in an sbottom cascade; the top quark and the chargino. An SSDL pair originates from two W -bosons of the same sign that would come from the cascades of the $\tilde{b}\tilde{b}^*$ pair originally produced in the hard scattering. Being known to be a very clean search channel, the SSDL final state offers an efficient probe to the sbottom sector. From the above discussion it is apparent that, in our scenario, this could only be the case if \tilde{b}_1 is dominantly L-type thus attracting the bound mentioned above.

Here, we would like to make a very general observation (valid in the MSSM as well) which is, to the best of our knowledge, new. In a setup with lighter higgsino-like neutralinos and chargino (the lightest states in case of the MSSM), there could be a region of phase space where the two-body decay $\tilde{b}_1 \rightarrow t\chi_1^-$ is closed but the three-body decays $\tilde{b}_1 \rightarrow tW^-\chi_1^0$ (via off-shell chargino) and/or $\tilde{b}_1 \rightarrow bW^+\chi_1^-$ (via off-shell top), which exploit(s) the same enhanced coupling \tilde{b}_1 - t - χ_1^- could compete and, under favorable circumstances (at low virtuality), beat the two-body $\tilde{b}_1 \rightarrow b\chi_{2,3}^0$ decay rate.

The phenomenon is illustrated in figure 1 in our NMSSM scenario with a light sbottom which is dominantly L-type. It shows the variations of decay branching fractions of \tilde{b}_1 in various 2- and 3-body decay modes as functions of $\Delta m(\tilde{b}_1, t + \chi_1^-)$, i.e., the difference of mass of \tilde{b}_1 and the sum of the masses of the top quark and the lighter chargino. $\Delta m(\tilde{b}_1, t + \chi_1^-)$ is

²While the present work is being finalized, The ATLAS Collaboration [46] has come up with some tighter lower bounds on the masses of stop and sbottom squarks from the 13 TeV run of the LHC under similar sets of theoretical assumptions. This might have some limited numerical bearing on the present work. We, however, continue to use the analyses of references [1, 2] which are incorporated and validated in a popular framework like `CheckMATE` [47, 48]. The analyses discussed here and the conclusions drawn thereof are expected to remain broadly unaltered when subjected to the latest experimental results.

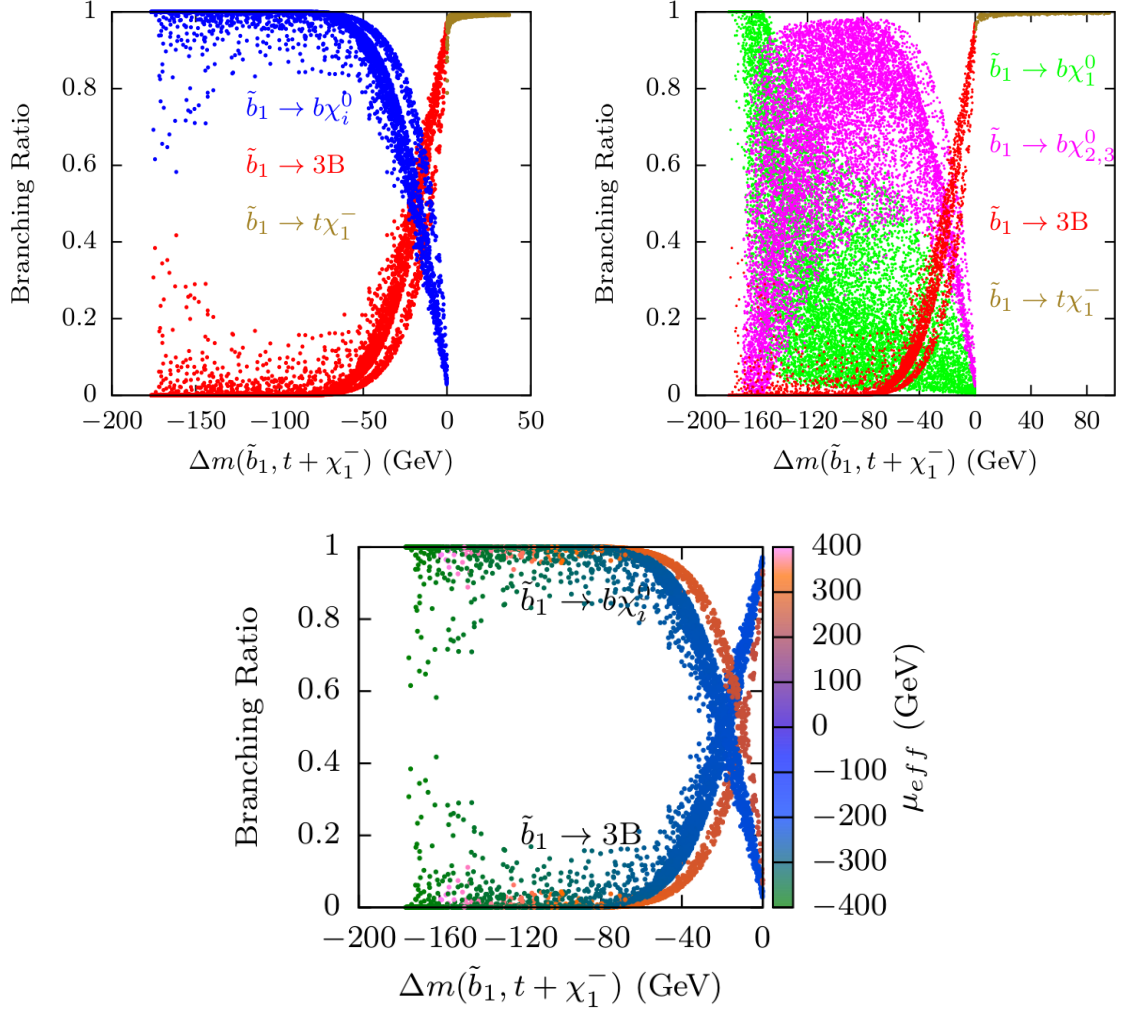


Figure 1. Variations of branching fractions of \tilde{b}_1 into various two- and three-body decay modes as functions of $\Delta m(\tilde{b}_1, t + \chi_1^-)$ with μ_{eff} being indicated in the color palette. The scan is performed with $1 < \tan \beta < 3$, $0.6 < \lambda < 0.75$, $0.01 < \kappa < 0.4$, $100 < |\mu_{\text{eff}}| < 400$ GeV, $|A_{\lambda, \kappa}| < 1$ TeV, $m_{\tilde{Q}_3} = 570$ GeV, $m_{\tilde{U}_3} = m_{\tilde{D}_3} = 1500$ GeV and $A_{t,b} = 0$, $M_1, M_2 = 1$ TeV and $M_3 = 2$ TeV. The value of $m_{\tilde{b}_1}$ is fixed around 400 GeV. Only those points are chosen for which the singlino fraction in the LSP is larger than 50%. ‘3B’ stands for 3-body decays. See text for further details.

varied by varying μ_{eff} which is reflected in the color palette. The scatter plot on the left of the upper panel shows how the 3-body decay branching ratio (in red) takes off significantly in advance of the 2-body threshold of $\tilde{b}_1 \rightarrow t\chi_1^-$ (in light brown) and how it overtakes the collective 2-body branching ratio into $b\chi_{1,2,3}^0$ final states (in blue). This then indicates the onset of the regime where bounds from both $\tilde{b}_1 \rightarrow b$ LSP and $\tilde{b}_1 \rightarrow t\chi_1^-$ cease to exist. The right plot of the upper panel reveals that the $\text{BR}[\tilde{b}_1 \rightarrow b\chi_{2,3}^0]$ has the dominant share in the collective 2-body branching ratio over most of the parameter space. The 2-body branching ratio for the decay $\tilde{b}_1 \rightarrow b\chi_1^0$ (singlino) is mostly small and only becomes significant when

Δm is large negative thus implying the decays $\tilde{b}_1 \rightarrow b\chi_{2,3}^0$ suppressed by phase space.

Our goal is to find how light the sbottom could be under such a circumstance. We thus choose an sbottom mass of 400 GeV for the illustration. This is close to but smaller than the current bound of around 470 GeV obtained assuming $\text{BR}[\tilde{b}_1 \rightarrow t\chi_1^-]=100\%$. A good check to ensure that such a relaxation is indeed possible is to subject the parameter point to a **CheckMATE** analysis. We find that this is indeed the case. In principle, under such a circumstance, an even lighter sbottom could have escaped the current experimental searches.

In any case, it is important to realize that such a light $\tilde{b}_1 \equiv \tilde{b}_L$ would imply a nearby light stop. The latter could generically escape the latest LHC bounds obtained assuming $\tilde{t}_1 \rightarrow t\chi_1^0$ or $\tilde{t}_1 \rightarrow b\chi_1^-$ only if it shares its decay branching fractions among available modes [1, 2]. This, in turn, is possible in two ways: first, if there is some mixing present in the stop sector leading to some admixture of R-type stop in a predominantly L-type \tilde{t}_1 ; secondly, even for an unmixed L-type \tilde{t}_1 if it could decay to heavier neutralinos.

A careful look at the left plot of the upper panel of figure 1 reveals a narrow slit within the red and the blue bands. The plot in the bottom panel reveals that the slits actually separate two strands which have $\mu_{\text{eff}} < 0$ (in blue) and $\mu_{\text{eff}} > 0$ (in orange). A priori, this may not be unusual given that the sign on μ_{eff} is known to affect phenomenology in a modest way [15]. In fact, we found that the 3-body decay widths of \tilde{b}_1 remain comparable for either sign of μ_{eff} in the regime under consideration. Rather, the slits have their origin in the palpably different 2-body decay widths of \tilde{b}_1 for negative and positive μ_{eff} , the latter resulting in a larger width. This effect, in turn, can be traced back to different couplings of sbottoms to the gaugino components of the light neutralino states for the two signs on μ_{eff} . Note that even though we work in a regime where $\mu_{\text{eff}} \ll M_1 = M_2$ (=1.5 TeV), i.e., in a somewhat ‘deep higgsino region’, a suppressed bottom Yukawa coupling (as is expected for low values of $\tan\beta$) makes way for even small gaugino admixtures to play the lead role. Indeed, this effect can be minimized by increasing the values of M_1 and M_2 further. Also note that, the small values of Δm on the left part of the plot indeed correspond to large μ_{eff} (mostly negative) and hence to a heavier chargino.

The Feynman diagrams of the two possible modes of 3-body decay of sbottom are shown in figure 2: $\tilde{b}_1 \rightarrow tW^-\chi_1^0$ proceeds through a virtual χ_1^- while $\tilde{b}_1 \rightarrow bW^+\chi_1^-$ proceeds through a virtual top quark. The former is dominant at low values of Δm for which the chargino is heavier. The latter dominates for low values of μ_{eff} where the 3-body final state competes with the 2-body one.

It turns out, however, that the scattered points in the left part of these plots with the 3-body decays reaching up to $\sim 40\%$ cannot survive bounds from stop searches at the LHC. This is because for these points the LSP is relatively light (~ 50 GeV) and thus $\text{BR}[\tilde{t}_1 \rightarrow t \text{LSP}]$ could still be 100% even though the LSP is mostly singlino-dominated (since κ is small and μ_{eff} is large) thanks to the large top Yukawa coupling. Also, since $\mu_{\text{eff}} \approx m_{\tilde{b}_1} \approx m_{\tilde{t}_1} \sim 400$ GeV (both \tilde{b}_1 and \tilde{t}_1 being dominantly L-type) and thus the chargino is very close to the stop mass, the 2-body decays of stop to higgsino-like states would be suppressed. Given the nature of the couplings there could be a competition among various decay modes of stop. An appropriate LHC study on the stop sector [2] rules these points out.

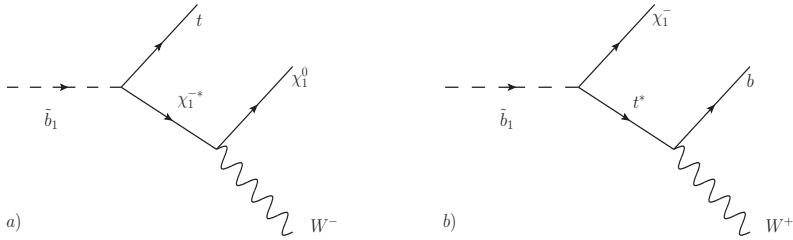


Figure 2. Feynman diagrams representing 3-body decays of \tilde{b}_1 .

In the context of the NMSSM, it is particularly noteworthy that published LHC results [2] do not constrain $m_{\tilde{b}_1}$ at all when $m_{\tilde{\chi}_2^0} \lesssim 280$ GeV for both $\text{BR}[\tilde{b}_1 \rightarrow b\tilde{\chi}_2^0]$ and $\text{BR}[\tilde{\chi}_2^0 \rightarrow \tilde{\chi}_1^0 h]$ being 100%. Presence of a singlino-like LSP in the spectrum and a pair of, rather degenerate, higgsino-like neutralinos could naturally fulfil such conditions in the cascade decay of $\tilde{b}_1 \equiv \tilde{b}_L$ if its decay to the $t\tilde{\chi}_1^-$ final state is not only kinematically disallowed but $m_{\tilde{b}_1}$ is also significantly below the $t\tilde{\chi}_1^-$ threshold (see section 3.3).

3.2 The case with a light $\tilde{b}_1 \equiv \tilde{b}_R$

The important difference between the phenomenology of $\tilde{b}_1 \equiv \tilde{b}_R$ and that of $\tilde{b}_1 \equiv \tilde{b}_L$ is that all the relevant decays of \tilde{b}_R to higgsino-like states are governed by the small bottom Yukawa coupling and thus they all compete and saturate above the top-chargino threshold. This is shown in figure 3. When compared to figure 1, a sharp contrast is clearly visible in the vicinity of the bottom-chargino threshold and beyond. Note that while for \tilde{b}_L the decay to the chargino final state quickly dominates and becomes 100% above the threshold, the same for \tilde{b}_R saturates to a value of around 40%.

As a result, in this regime, bound on a light sbottom, which is R-type, obtained from the top-chargino mode would be much relaxed when compared to the case of an L-type sbottom. In practice, the amount of such a relaxation can only be estimated explicitly using a framework like **CheckMATE**. On the theoretical side, under such a situation, the lower bound on the mass of the \tilde{b}_R is restricted by how low one could go down in the chargino mass. The latter is constrained by LHC analyses involving the chargino-LSP system when the chargino decays 100% of the times to W -LSP, which is the case in the NMSSM scenario we are discussing. References [49, 50] indicate that under such a situation chargino mass as low as 200 GeV is allowed³ for a LSP mass around 100 GeV.

3.3 The case with $m_{\tilde{b}_1} < m_t + m_{\tilde{\chi}_1^-}$

Issues with sbottom having mass below the top-chargino threshold (large μ_{eff}) are more or less similar for \tilde{b}_L and \tilde{b}_R . The important exception is that for the latter case the 3-body decays are not at all favored below the top-chargino threshold. In both cases, the two body

³It has recently been reported in [51] that mass-reaches like $m_{\tilde{\chi}_{2,3}^0, \tilde{\chi}_1^\pm} \sim 320(500)$ GeV are possible for the current 13 TeV, 30 fb⁻¹ (future 14 TeV, 300 fb⁻¹) run of the LHC. Thus, masses for these excitations that are used in most of the benchmark points are within the reach of 13 TeV LHC run.

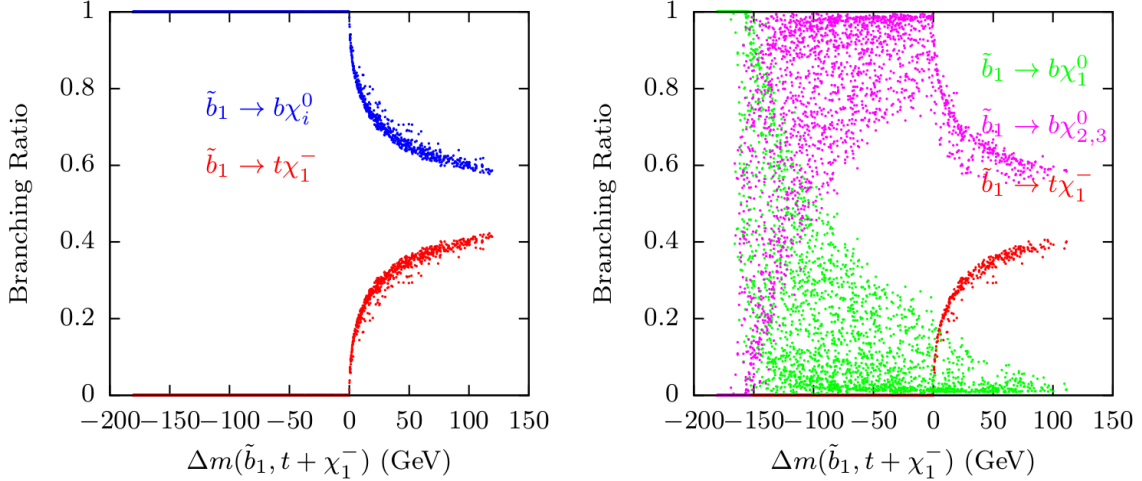


Figure 3. Same as in the plots in the upper panel of figure 1 but for an R-type \tilde{b}_1 .

decays to $b\chi_i^0$ dominate. In this regime, it is, however, important to study how these latter BRs are shared among b -LSP (χ_1^0 ; singlino-like) and $b\chi_{2,3}^0$ (higgsino-like) since these rates determine which kind of experimental constraints on sbottom mass would be pertinent. It can be noted here that sbottoms are searched for at the LHC assuming their three pure modes of decays, viz., $\tilde{b}_1 \rightarrow b\chi_1^0$, $\tilde{b}_1 \rightarrow b\chi_2^0$ followed by $\chi_2^0 \rightarrow h\chi_1^0$ and $\tilde{b}_1 \rightarrow t\chi_1^-$ [26, 28]. For sbottom mass below the top-chargino threshold the last decay mode simply does not exist.

In the right plot of the upper panel of figure 1 and in the right plot of figure 3 we illustrate these shares of BRs for \tilde{b}_L and \tilde{b}_R , respectively. As before, the outer edges of the green and the pink regions correspond to the maximum admixture (50%) of higgsino in the LSP that we allow for in this analysis. The figures show that BR in bottom-LSP drops sharply as μ_{eff} decreases (as we go from left to right) since this opens up the decays to $b\chi_{2,3}^0$. Clearly, thus, the bounds on sbottom mass that assume $\text{BR}[\tilde{b}_1 \rightarrow b \text{ LSP}] = 100\%$ would not hold in this regime. The next regime with $\text{BR}[\tilde{b}_1 \rightarrow b\chi_{2,3}^0] = 100\%$, where sbottom searches put bound on its mass, also gets affected because of such a sharing of branching fractions thus resulting in a relaxed bound. The situation is a bit worse for \tilde{b}_L for which the 3-body decays also get their shares in this regime.

3.4 Effect of mixing in the sbottom sector

The discussions in section 3.1 could well point to how things change drastically even for a small admixture of \tilde{b}_L in an otherwise \tilde{b}_R -dominated \tilde{b}_1 . It may be reiterated that, unlike in the case of the MSSM, one could afford a significantly low $\tan\beta$ (~ 2) in the NMSSM when λ is large. As a consequence, $\frac{y_t}{y_b}$ could become large. Given that the mixing in the sbottom sector is naturally restrained, it is all the more interesting to observe how significantly this affects the decay pattern of \tilde{b}_1 having only very small \tilde{b}_L admixture.

In the left plot of figure 4 we illustrate the implication of such a small \tilde{b}_L -admixture in \tilde{b}_1 for the decay branching fraction $\text{BR}[\tilde{b}_1 \rightarrow t\chi_1^-]$. We take close values of $m_{\tilde{Q}_3}$ (~ 680 GeV)

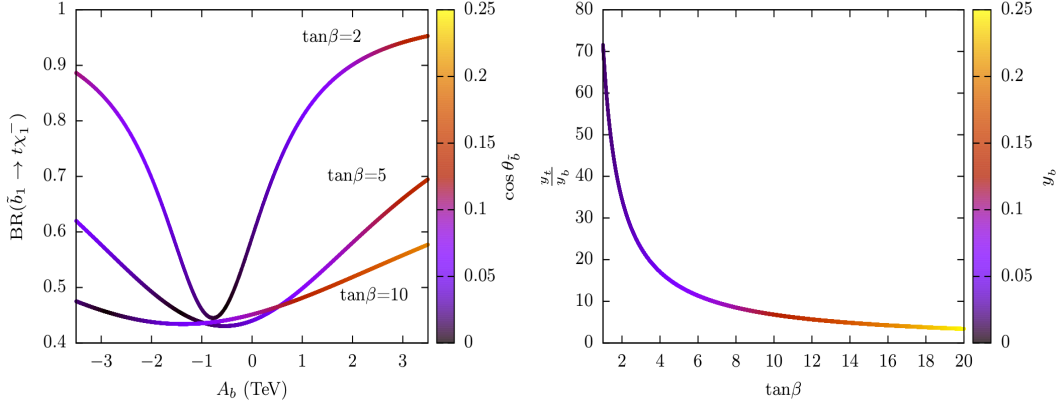


Figure 4. **Left:** Variations of $\text{BR}(\tilde{b}_1 \rightarrow t\chi_1^-)$ as a function of A_b for various values of $\tan\beta$. The color palette indicates the varying magnitude of sbottom mixing along each curve in terms of $\cos\theta_{\tilde{b}}$. Other parameters are fixed as follows: $\mu_{\text{eff}} = -300$ GeV, $m_{\tilde{b}_1} \approx 700$ GeV, $m_{\tilde{b}_2} \approx 750$ GeV, $m_{\tilde{Q}_3} = 680$ GeV, $m_{\tilde{U}_3} = 1.5$ TeV, $m_{\tilde{D}_3} = 630$ GeV, $A_t = 0$, $M_1 = 1$ TeV, $M_2 = 1.5$ TeV and $M_3 = 2$ TeV. **Right:** Variation of the ratio $\frac{y_t}{y_b}$ as a function of $\tan\beta$. The color palette indicates the varying magnitude of y_b along the curve.

and $m_{\tilde{D}_3}$ (~ 630 GeV) which facilitate mixing in the sbottom sector. Also, we fix μ_{eff} at -300 GeV, a value which is representative of a ‘natural’ setup. Variations of colour along the individual curves reflect the varying chiral-mixing (in terms of $\cos\theta_{\tilde{b}}$) which can be gleaned from the colour palette. Note that $\cos\theta_{\tilde{b}} = 0$ implies a pure R-type \tilde{b}_1 (see section 2.1).

Variations of $\text{BR}[\tilde{b}_1 \rightarrow t\chi_1^-]$ are then shown for three representative values of $\tan\beta$ ranging over small to intermediate values. It can be seen from the figure that for all values of $\tan\beta$, the said branching fraction increases with increasing $|A_b|$. This is expected since increasing A_b can indeed induce larger \tilde{b}_L admixture in \tilde{b}_1 which is predominantly R-type in our present setup. The positions of the troughs in all these curves are primarily determined by the values of A_b for which the \tilde{b}_L admixtures are the smallest. For small $\tan\beta$ (≈ 2), this can be clearly seen in the figure. The relative locations of the troughs for curves with different values of $\tan\beta$, however, have complicated dependence on both A_b and $\tan\beta$. Also, one could find that, for large values of $|A_b|$, $\text{BR}[\tilde{b}_1 \rightarrow t\chi_1^-]$ could get as large as 95%, 70% and 55% for $\tan\beta = 2, 5$ and 10, respectively with a small to moderate mixing. Furthermore, one can see that the gradients of the variations are steeper for smaller $\tan\beta$ values. This can be seen as a result of how the ratio $\frac{y_t}{y_b}$ varies as a function of $\tan\beta$. This variation is shown in the right plot of figure 4.

Such large branchings of \tilde{b}_1 to top quark and chargino, under the present setup, are definite outcomes of possible low values of $\tan\beta$ which can be easily accommodated in a ‘natural’ NMSSM scenario. In contrast, in the MSSM, such a large branching fraction for $\tilde{b}_1 \rightarrow t\chi_1^-$ is rather difficult to attain since the observed mass of the SM-like Higgs boson restricts $\tan\beta$ from the bottom.

4 Benchmark scenarios and the 13 TeV LHC

As has been already pointed out, studying the phenomenology of sbottoms is important in its own right and could shed crucial light on the physics of the squarks from the third generation by complementing/supplementing the studies in the stop sector. The subject gets further involved in nontrivial ways in a scenario like ‘natural’ NMSSM, in particular, in the light of available results from the LHC Run-I. A systematic first study into this should be based on some salient aspects that the sbottom sector possesses in such a setup. Some such issues are discussed in the previous section. In this section we first present a few benchmark points which are representative of the situations described in sections 3.1, 3.2 and 3.4. We then study the collider aspects of these scenarios at the ongoing LHC-13.

4.1 Benchmark scenarios

In table 1 we present six benchmark scenarios/points (BPs). For all of them, we fix the gaugino soft mass parameters to be $M_1 = 1$ TeV, $M_2 = 1.5$ TeV and $M_3 = 2$ TeV such that the heavier neutralinos and the heavier chargino are absent in the cascades of a much lighter \tilde{b}_1 (a simplified scenario with only singlino- and higgsino-like lighter neutralinos and a higgsino-like lighter chargino). Large values of λ ($\gtrsim 0.6$) are chosen in order to enhance the tree level NMSSM contribution to the SM-like Higgs boson mass. As discussed earlier, this requires low values of κ to ensure the absence of Landau pole below the GUT scale which, in turn, results in an LSP which is singlino-like. We thus choose $\kappa \lesssim 0.25$. Except for BP6, all other benchmark points have $A_t = 0$, as discussed in section 3.1.

Two common but salient features of these scenarios are that they all have small $\tan\beta$ (~ 2) and that the LSP is mostly a singlino ($\sim 75\% - 90\%$), albeit with a non-negligible higgsino admixture. Such a composition is achieved by choosing relatively large values of λ ($\gtrsim 0.6$) while keeping μ_{eff} somewhat smaller. Note that such a setup generically guarantees a low fine-tuning (i.e., more ‘natural’) and singlino-domination in the LSP can thus be seen to be directly connected to this fact. Palpable mixing among the higgsino and the singlino states is also unavoidable for large λ and since $\mu_{\text{eff}} \approx \lambda v_S$ is a possibility. The benchmark scenarios presented here are checked for their viability via **CheckMATE** against the available analyses of the LHC Run-I data. These points also satisfy all Higgs-related constraints and other phenomenological bounds that are built-in in **NMSSMTools-v4.8.2** [52–56]. However, constraints pertaining to muon $g - 2$ are ignored while in the dark matter sector only the upper bound on the relic density ($\Omega_c h^2 < 0.131$) as incorporated in **NMSSMTools** is respected.

We have presented three benchmark scenarios (BP1-BP3) having \tilde{b}_1 which is purely \tilde{b}_R while for the scenarios BP5 and BP6 it is purely \tilde{b}_L . In BP4 we allow for a little admixture of \tilde{b}_L in \tilde{b}_1 . Scenarios BP1 and BP2 differ in the masses of \tilde{b}_1 and in the fact whether h_1 or h_2 is the SM-like Higgs boson. BP2 and BP3 are rather similar except for the possibility of an additional decay of $\chi_{2,3}^0$ to h_1 that is available for the latter. For these three benchmark points we set $m_{\tilde{Q}_3} = m_{\tilde{U}_3} = 1500$ GeV⁴ and appropriately small values of $m_{\tilde{D}_3}$ are chosen.

⁴Choice of stops and an sbottom as heavy as 1.5 TeV, whenever possible, is made just to ensure that

In BP4 we present a scenario where a small admixture of \tilde{b}_L in $\tilde{b}_1 (\simeq \tilde{b}_R)$ which is achieved by making A_b large even as $m_{\tilde{Q}_3} \sim m_{\tilde{D}_3}$. As pointed out earlier, even a tiny left admixture ($\lesssim 2\%$), when assisted by large $\frac{y_t}{y_b}$ (driven by small $\tan\beta$), could result in a very large branching fraction for $\tilde{b}_1 \rightarrow t\chi_1^+$ (reaching $\sim 90\%$). This is something not usually expected of $\tilde{b}_1 \equiv \tilde{b}_R$, in particular, when other two-body decay modes (to light neutralinos) are kinematically accessible to it.

In BP5 \tilde{b}_1 is made to resemble \tilde{b}_L by lowering the $m_{\tilde{Q}_3}$ ($=500 \text{ GeV} \ll m_{\tilde{U}_3} = m_{\tilde{D}_3} = 1500 \text{ GeV}$). BP6 is a point representative of the cross-over region for the curves that illustrate the variations of the 2-body and 3-body branching fractions of \tilde{b}_1 in figure 3. Note that, in this case, the lighter stop has a mass of around 400 GeV. As pointed out in section 3.1, this could escape the latest bound from the LHC only if the stop sector is attributed with some mixing. Also, BP6 features sub-TeV \tilde{t}_1 and \tilde{t}_2 whose origins are discussed in section 3.1.

As far as the cascades of the light neutralinos and the lighter chargino are concerned, it can be seen from table 1 that the former decay predominantly to $\chi_1^0 Z$ followed by $\chi_1^0 h$ (SM-like) while the latter decays 100% of the time to $\chi_1^0 W^\pm$. Scenario BP5 is an exception for which $\text{BR}[\chi_2^0 \rightarrow \chi_1^0 h]$ dominates over $\text{BR}[\chi_2^0 \rightarrow \chi_1^0 Z]$. For all the benchmark points, current bounds on the chargino-neutralino and the third generation squark sectors are respected, using the public software `CheckMATE` wherever dimmed necessary.

4.2 Sbottoms at the LHC-13

In table 2 we present the possible decay modes of the sbottoms and the stops and indicate the intermediate products in the cascades and the partonic final states thereof. It may be apparent from the table that a simultaneous analysis involving various multi-lepton ($n_\ell \geq 3$) and SSDL final states with low b -jet multiplicity may be a useful probe to such a scenario. The cascade decays of stops could yield a larger b -jet multiplicity. This might eventually help recognizing the presence of stops. In all these cases the leptons have their origins in the decays of the SM gauge bosons. The cascade of higgsino-like neutralino will vary crucially determine the signal topology. Identifying b -jets will certainly be helpful in this specific scenario. Table 4 describes suitable cuts for the above mentioned signal topologies.

The SSDL signal arises only from the cascade $\tilde{b}_1 \rightarrow t\chi_1^-$ followed by $\chi_1^- \rightarrow \chi_1^0 W^-$. The pure L-type stop quark will never give an SSDL signal in this set up. So the observation of the SSDL signal would definitely point to a \tilde{b}_1 cascade. But as we can see from BP4, due to the effect of large $\frac{y_t}{y_b}$, it may not be easy to estimate the mixing in the sbottom sector.

they effectively decouple for our purpose while the other sbottom may still remain light in the scenario under consideration. It may, however, be noted that stops with mass $\lesssim 1 \text{ TeV}$ would not affect yields in the final states we consider and, hence our results, in any significant way. As discussed in the Introduction, relatively heavier stops may not necessarily be in conflict with ‘naturalness’ when $|\mu_{eff}|$ is small enough. This has been checked explicitly by using `NMSSTools` where the related finetuning parameter yields values ~ 10 , which is indicative of a healthy naturalness, for all the benchmark points with heavy stop(s).

Parameters	BP1	BP2	BP3	BP4	BP5	BP6
λ	0.63	0.65	0.65	0.67	0.68	0.70
κ	0.15	0.20	0.17	0.20	0.19	0.25
A_λ (GeV)	435	-600	-600	-580	660	-320
A_κ (GeV)	-50	50	50	50	-50	85
μ_{eff} (GeV)	200	-300	-300	-300	350	-250
$\tan\beta$	2	2	2	2	2	1.6
A_t (GeV)	0	0	0	0	0	300
A_b (GeV)	-1000	-1000	-1000	-2500	0	0
$m_{\tilde{Q}_3}$ (GeV)	1500	1500	1500	550	500	260
$m_{\tilde{U}_3}$ (GeV)	1500	1500	1500	1500	1500	400
$m_{\tilde{D}_3}$ (GeV)	330	440	440	520	1500	1500
Observables	BP1	BP2	BP3	BP4	BP5	BP6
Singlino fraction in the LSP	0.78	0.87	0.90	0.87	0.89	0.77
\tilde{b}_R fraction in \tilde{b}_1	1	1	1	0.98	0	0
m_{h_1} (GeV)	107.1	124.4	125.7	124.6	123.2	125.9
m_{h_2} (GeV)	125.2	190.2	163.8	184.4	202.6	173.1
$m_{\tilde{b}_1}$ (GeV)	407.7	506.0	506.0	598.3	588.5	405.0
$m_{\tilde{b}_2}$ (GeV)	1553.3	1552.4	1552.4	633.9	1557.6	1549.0
$m_{\tilde{t}_1}$ (GeV)	1552.8	1555.1	1555.1	650.0	605.6	396.2
$m_{\tilde{t}_2}$ (GeV)	1567.4	1564.5	1564.5	1556.7	1557.2	533.6
$m_{\chi_1^0}$ (GeV)	113.7	200.1	171.7	194.3	209.5	195.1
$m_{\chi_2^0}$ (GeV)	212.0	322.0	319.6	319.5	356.0	264.0
$m_{\chi_3^0}$ (GeV)	238.3	328.2	329.2	327.1	376.0	274.4
$m_{\chi_1^-}$ (GeV)	201.0	309.2	309.2	306.4	348.8	250.0
$\text{BR}(\tilde{b}_1 \rightarrow t\chi_1^-)$	0.29	0.30	0.30	0.93	1	0
$\text{BR}(\tilde{b}_1 \rightarrow b\chi_1^0)$	0.02	0.01	0	0	0	0.18
$\text{BR}(\tilde{b}_1 \rightarrow 3\text{-body})$	0	0	0	0	0	0.57
$\text{BR}(\tilde{b}_2 \rightarrow t\chi_1^-)$	0.73	0.76	0.76	1	0	0
$\text{BR}(\chi_2^0 \rightarrow \chi_1^0 Z)$	1	1	0.65	0.85	0.40	0.95
$\text{BR}(\chi_2^0 \rightarrow \chi_1^0 h)$	0	0	0.35	0.15	0.60	0
$\text{BR}(\chi_3^0 \rightarrow \chi_1^0 Z)$	1	0.99	0.79	0.96	0.80	0.98
$\text{BR}(\chi_3^0 \rightarrow \chi_1^0 h)$	0	0.01	0.21	0.04	0.20	0

Table 1. Benchmark points studied in the present work. The slepton and the first two generation squark masses are all set to 1.5 TeV and the $SU(3)$ gaugino mass, M_3 is set to 2 TeV. The $SU(2)$ gaugino mass M_2 is set to 1.5 TeV and $U(1)_Y$ gaugino mass M_1 is set to 1 TeV. Remaining sbottom branching fraction in each case is attributed to its decays to $b\chi_{2,3}^0$. See text for details.

Cascade modes	Intermediate products	Partonic final states
$\tilde{b}_1 \rightarrow b\chi_{2,3}^0, \tilde{b}_1 \rightarrow b\chi_{2,3}^0$	$2b + 2(Z/h)$	$4\ell + 2b + \cancel{E}_T$
$\tilde{b}_1 \rightarrow t\chi_1^-, \tilde{b}_1 \rightarrow b\chi_{2,3}^0$	$2b + W^+W^- + (Z/h)$	$(3\ell, 4\ell) + 2b + \cancel{E}_T$
$\tilde{b}_{1,2} \rightarrow t\chi_1^-, \tilde{b}_{1,2} \rightarrow t\chi_1^-$	$2b + 2(W^+W^-)$	$(\text{SSDL}, 3\ell, 4\ell) + 2b + \cancel{E}_T$
$\tilde{t}_{1,2} \rightarrow t\chi_{2,3}^0, \tilde{t}_{1,2} \rightarrow t\chi_{2,3}^0$	$2b + W^+W^- + 2(Z/h)$	$(3\ell, 4\ell) + 4b + \cancel{E}_T$
$\tilde{t}_{1,2} \rightarrow t\chi_{2,3}^0, \tilde{t}_{1,2} \rightarrow b\chi_1^+/t\chi_1^0$	$2b + W^+W^- + Z/h$	$(3\ell, 4\ell) + 2b + \cancel{E}_T$

Table 2. Possible decay modes of $\tilde{b}_{1,2}, \tilde{t}_{1,2}$. The decays $\chi_{2,3}^0 \rightarrow \chi_1^0 Z/h$ and $\chi_1^- \rightarrow W^- \chi_1^0$ have 100% branching fraction.

Channel ID	Search channel	Dominant backgrounds
SRSSDL	$\text{SSDL}+ \geq 2j(2b) + \cancel{E}_T$	$t\bar{t}, t\bar{t}Z, t\bar{t}W$
SR3l2b	$3\ell+ \geq 4j(2b) + \cancel{E}_T$	$t\bar{t}, t\bar{t}Z, t\bar{t}W$
SR4l1b	$3\ell+ \geq 2j(1b) + \cancel{E}_T$	$t\bar{t}Z, t\bar{t}W$

Table 3. Classification of signal regions in terms of the actual search channels undertaken in the present analysis. Leptons have their origins in the Z - and the W -bosons. The last column presents the dominant SM background processes corresponding to each final state. These are inclusive of two hard jets except for the ZW and $t\bar{t}$ processes for which three-jet inclusive samples are used.

4.3 Simulation setup and selection of final states

The lowest order (LO) parton-level signal events are generated using `MadGraph_aMc@NLO v2.3.3` [57]. Background events are obtained using `MadGraph_aMc@NLO v2.1.2` [57]. In both cases, parton distribution function `nn23lo1` [58], default to `MadGraph`, is used with the factorization/renormalization scale set at the default `MadGraph` setting of transverse mass. For the signal, the next-to-leading-order (NLO) cross sections are estimated via `Prospino v2.1` [59]. For the backgrounds, to take into the account higher order effects, we employ a flat K -factor of 1.6 for the inclusive $t\bar{t}$ samples and 1.3 for the rest.

Signal events are showered with `Pythia v8.2` [60]. Background events are showered with `Pythia v6.426` [61] embedded in the `MadGraph` setup. For background events, we employ the MLM [62, 63] scheme for matching jets in order to avoid double counting in the presence of hard partonic jets and parton shower. Background events are produced with up to three inclusive jets.

Subsequently, both signal and background events are subjected to detector simulation

via DELPHES v3.2.0 [64] which includes Fastjet v3.1.0 [65] for jet reconstruction. For merging of jets, we employ the anti- k_T algorithm with cone size set to 0.4 and require a minimum p_T^{jet} of 20 GeV with pseudorapidity in the range $|\eta_{jet}| < 2.5$. b -tagging efficiency is set to 70%. Furthermore, we consider the probability of a c -jet and a light quark jet being tagged as a b -jet to be 20% and 1%, respectively.

Leptons (electrons and muons) are reconstructed with minimum p_T^ℓ of 10 GeV and with $|\eta_\ell| < 2.5$. Leptons having neighbouring (reconstructed) jets lying within a cone of $\Delta R \leq 0.2$ about them are rejected. To increase the purity of electrons further, we require the ratio of total p_T of the stray tracks within the cones of their identification to their own p_T 's is less than 0.1. For muons the maximum total p_T of other tracks is required to be below 1.8 GeV.

Variables	SRSSDL	SR3 ℓ 2b	SR4 ℓ 1b
n_ℓ	2 (SSDL)	3	4
n_{jet}	≥ 2	≥ 4	≥ 2
n_{b-jet}	≥ 2	≥ 2	≥ 1
$p_T^{j(n)}$ (GeV) $p_T^{b-jet(n)}$ (GeV)	$p_T^{j(1,2,3,\geq 4)} > (30, 30, 30, 20)$ $p_T^{b-jet(1,2)} > (40, 30)$		
p_T^ℓ (GeV)	$p_T^{\ell(1,2,3,4)} > (30, 20, 15, 15)$		
\cancel{E}_T (GeV)	> 100		
m_{T2} (GeV)	> 90	-	-
H_T (GeV)	> 400	> 500	> 500

Table 4. Definitions of the signal regions (SR) indicating the final states they represent and the sets of selection cuts on the physics objects that are independent of the benchmark scenarios. By leptons only electrons and muons are referred to. Other notations follow standard conventions.

In table 4 we define three distinct signal regions namely SRSSDL, SR3 ℓ 2b and SR4 ℓ 1b and the signal selection cuts used for them in the framework of MadAnalysis 5v1.1.12 [66–68]. Jets and leptons are p_T -ordered with the hardest jet being denoted as j_1 and the hardest lepton as ℓ_1 . To have a better handle on some important backgrounds like $t\bar{t} + jets$, we employ standard kinematic variables like $H_T = \sum_{jets} |p_T^j|$ and m_{T2} [69], where

$$m_{T2}(p_T^{\ell_1}, p_T^{\ell_2}, \not{p}_T) = \min_{\not{p}_{T,1} + \not{p}_{T,2} = \not{p}_T} \{ \max\{m_T(p_T^{\ell_1}, \not{p}_{T,1}), m_T(p_T^{\ell_2}, \not{p}_{T,2})\} \} \quad (4.1)$$

with

$$m_T(p_T^\ell, \not{p}_T) = \sqrt{2p_T^\ell \not{p}_T (1 - \cos \phi_{\ell, \not{p}_T})} \quad (4.2)$$

4.4 Results and discussion

In this subsection we discuss the results of our simulations for the LHC-13 in different signal regions described in table 4. These signal regions satisfy a general set of cuts on lepton and jet

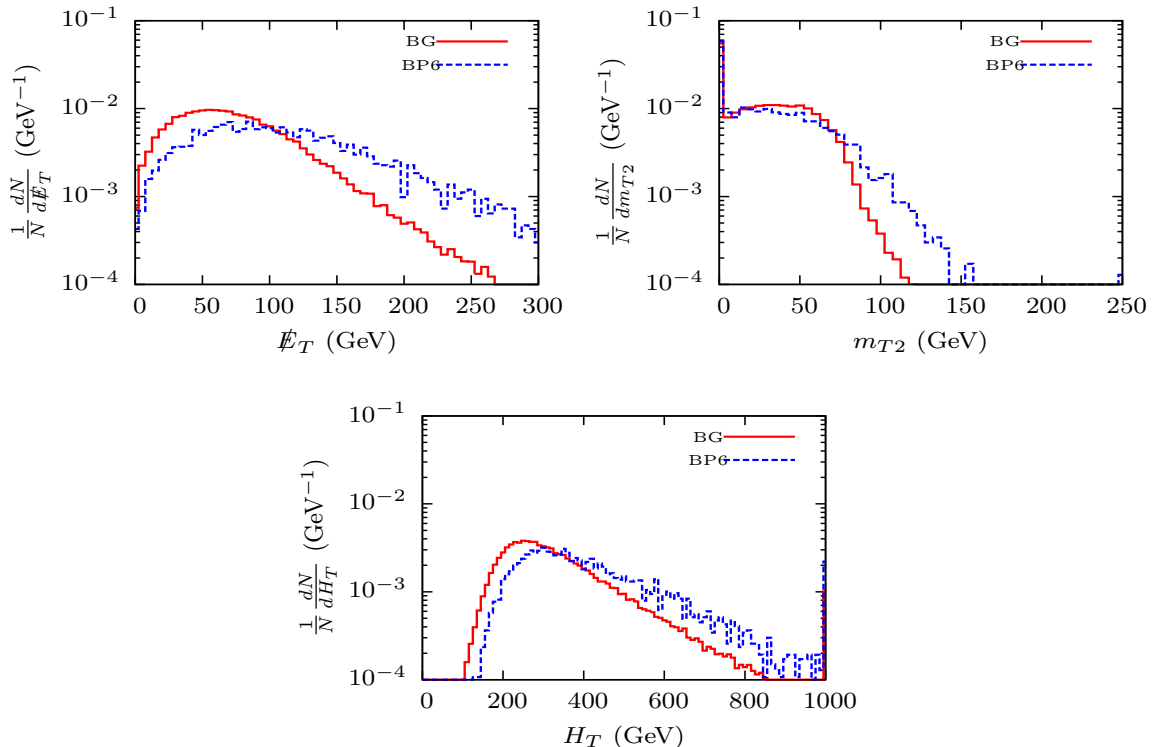


Figure 5. Differential distributions for the kinematic variables \cancel{E}_T , m_{T2} and H_T for both signal (in scenario BP6) and the background at LHC-13 for inclusive final states. See text for details.

p_T 's that are appropriate for the LHC-13 along with the multiplicities of the same (including b -jets) that characterize the concerned final states. In addition, these regions also feature cuts on kinematic variables like the missing transverse energy (\cancel{E}_T), m_{T2} and H_T which are chosen by studying the respective distributions as shown in figure 5. Note that the plots in figure 5 are obtained using the benchmark scenario (BP6) which, as we would find later (see table 5), shows a good sensitivity to the rather characteristic multi-lepton (> 2 leptons) final states. Furthermore, the set of kinematic cuts extracted from these distributions is also found to be optimal for other benchmark scenarios that we consider in this work.

We find that the LHC Run-I may not be generically sensitive to scenarios having somewhat low sbottom masses ($\lesssim 400$ GeV). The benchmark point BP1 having an R-type sbottom with mass ≈ 400 GeV, a near-degenerate pair of higgsino-like neutralinos (χ_2^0, χ_3^0) with $m_{\chi_{2,3}^0} \approx 200$ GeV and with an appreciable $\text{BR}[\tilde{b}_1 \rightarrow b\chi_{2,3}^0]$ is perfectly allowed by the recent LHC analyses. This is further confirmed through an explicit check using **CheckMATE**. Also, $\tilde{b}_1 \equiv \tilde{b}_L$ with mass ≈ 400 GeV (see scenario BP6) escapes the current bound that assumes $\text{BR}[\tilde{b}_1 \rightarrow b\chi_1^0]=100\%$. This is because in the present case, \tilde{b}_1 has shared branching fractions distributed among available two- and three-body decay modes, in all of which the final states are different from the one ($2b$ -jets + \cancel{E}_T) considered by the ATLAS collaboration [1, 2]. Note that while some such situations discussed in the framework of the MSSM are perfectly allowed departures from some simplifying assumptions, these are just the natural expectations in the

NMSSM in the presence of a light singlino-like LSP.

Benchmark scenario	Number of events and signal significance		
	SRSSDL	SR3 ℓ 2b	SR4 ℓ 1b
BP1	(88, 1200) < 2	(120, 146) 2.5	(120, 146) 9.0
BP2	(58, 47) < 2	(158, 1200) < 2	(56, 146) 4.4
BP3	(36, 47) < 2	(240, 1200) < 2	(37, 146) 3.0
BP4	(58, 47) 7.3	(158, 1200) 4.3	< 2
BP5	(36, 47) 4.7	< 2	< 2
BP6	< 2	(240, 1200) 6.7	(80, 146) 6.1

Table 5. Number of signal and background events after cuts (given in the parentheses, top sub-rows) and the corresponding signal significance (the bottom sub-row; for an integrated luminosity of 300 fb⁻¹) in different final states for the six benchmark points at the LHC-13.

Such NMSSM scenarios, however, can be studied at the LHC-13 in its early phase in various multi-lepton final states. The signal yields are presented in table 5 along with the corresponding expectations for the backgrounds for an integrated luminosity of 300 fb⁻¹. Also indicated in each case is the value of the signal-significance calculated using the Poisson distribution given by

$$\sigma = \sqrt{2 \left[(S + B) \ln\left(1 + \frac{S}{B}\right) - S \right]}. \quad (4.3)$$

To summarize, scenarios with $\tilde{b}_1 \equiv \tilde{b}_R$ (BP1, BP2 and BP3) are only sensitive to 4-lepton+*b-jet* (SR4 ℓ 1b) final state. Final states requiring three *b-jets* (e.g., SR3 ℓ 3b) are generally less promising irrespective of the scenarios considered. This is since the corresponding rates get suppressed by the extra *b-tag* efficiency factors. It should be stressed here that unravelling such a scenario would require corroborative signatures in multiple final states. Note that even with 300 fb⁻¹ of data, one could have not more than two simultaneous final states for which the signal significances reach 5σ (SRSSDL and SR3 ℓ 2b for scenario BP4 and SR3 ℓ 2b and SR4 ℓ 1b for scenario BP6).

In such scenarios with $\tilde{b}_1 \equiv \tilde{b}_R$, the SSDL final state is not at all sensitive since the decay $\tilde{b}_1 \rightarrow t\chi_1^-$ is heavily suppressed. For an R-type \tilde{b}_1 , its decay shares branching among the modes $\tilde{b}_1 \rightarrow b\chi_{2,3}^0$ significantly. For BP1 and BP2, the 4-lepton final states are reasonably sensitive as $\chi_{2,3}^0$ decays 100% of the times to $\chi_1^0 Z$ and leptons come from the decays of the *Z*-bosons. Still, the sensitivity is smaller for BP2 sheerly because of a heavier \tilde{b}_1 . On the

other hand, scenario BP3, in which decays of $\chi_{2,3}^0$ share branchings between $Z\chi_1^0$ and $h\chi_1^0$, naturally loses sensitivity to this final state.

Benchmark points BP5 and BP6 present the cases where $\tilde{b}_1 \equiv \tilde{b}_L$. For BP5, $\text{BR}(\tilde{b}_1 \rightarrow t\chi_1^-)$ is 100%. Naturally, as discussed earlier in section 3.1, the most sensitive final state is the one with SSDL. In BP6, we present a case where 3-body decays of \tilde{b}_1 (to $tW^-\chi_1^0$ and $bW^+\chi_1^-$) compete with its 2-body decays (to $b\chi_{1,2,3}^0$). This is the reason why BP6, albeit comes with an L-type \tilde{b}_1 , has a poor sensitivity in the SSDL final state. On the other hand, it has much better sensitivities in the 3-lepton and the 4-lepton final states.

It has been pointed out earlier that a relatively light L-type sbottom will always be accompanied by a (L-type) stop close-by in mass when the mixing in the stop sector is not large. In BP5 and BP6 we have such light \tilde{t}_1 -s which are not excluded by the usual stop-search as they share branchings among different decay modes like $t\chi_{1,2,3}^0$ and $b\chi_1^+$ [2]. Final states with high *b-jet* multiplicity like SR3 ℓ 3b and SR4 ℓ 3b are arising only from the stop cascade. We find that they are hardly significant with data worth 300 fb^{-1} .

In scenario BP4, \tilde{b}_1 and \tilde{b}_2 are close in mass. As we find, both of them decay dominantly to $t\chi_1^-$ with branching fractions larger than 90%. Note that this is a unique feature in the NMSSM and is in sharp contrast to the MSSM where, to obtain the mass of the SM-like Higgs boson in the right ballpark, $\tan\beta$ needs to be large and hence $\frac{y_t}{y_b}$ cannot become large enough to make both sbottoms decay dominantly to $t\chi_1^-$. Naturally, this scenario shows enhanced sensitivity ($\approx 7\sigma$) to the SSDL final state as both \tilde{b}_1 and \tilde{b}_2 contribute with similar strengths. This is clearly reflected in the signal corresponding significance as presented in table 5. In addition, BP4 is also found to be moderately sensitive to the 3 ℓ 2b final state.

It may be mentioned here that, in general, one may expect contributions to the final states under consideration from stop pair production as well. However, we find that except for BP6 these contributions are negligibly small. In BP6, it is \tilde{t}_2 that may contribute to 3- and 4-lepton final states but these do not exceed $\sim 25\%$.

A noteworthy omission in the list of final states is the canonical search mode involving $2b\text{-jets} + \cancel{E}_T$. An important upshot of such an NMSSM setup with a singlino dominated LSP is that a light sbottom, irrespective of its composition, would not generically have a healthy decay branching fraction to such an LSP. This would then deplete the event count in the $2b\text{-jet} + \cancel{E}_T$ final state severely while multi-lepton final states arising from the cascades of sbottom(s) via higgsino-like neutralinos would tend to dominate. In contrast to an MSSM scenario with small μ ($\sim \mu_{\text{eff}}$ and $\ll M_1, M_2$) thus having an LSP which is nearly mass-degenerate χ_2^0 (and χ_1^\pm), such cascades in a ‘natural’ NMSSM setup of the present kind could lead to leptons which are hard enough. As can be expected, the contrast becomes rather prominent when the decay $\tilde{b}_1 \rightarrow t\chi_1^-$ is kinematically forbidden.

In principle, such a depletion in the event rate in the $2b\text{-jets} + \cancel{E}_T$ final state, when contrasted against its expected rate in the MSSM, could be rather illuminating. This is best demonstrated in the variations of the effective branching fraction of a pair of sbottoms decaying to this final state in the NMSSM and in the MSSM. The spectral setup adopted for the purpose is shown in the left of figure 6 in the form of a level diagram. Note that, in the MSSM case, we deviate from the scheme with higgsino-like LSP described in the last

paragraph and introduce a bino-like LSP which can have some mixing with the higgsinos. This choice is rather conservative in the sense that it mimics the NMSSM spectrum thus allowing us to have a faithful estimate of the extent by which the signals from an analogous MSSM setup could masquerade as the NMSSM one. As is just pointed out, the mass-splitting between \tilde{b}_1 and the higgsino-like chargino is restricted to 150 GeV such that the decay $\tilde{b}_1 \rightarrow t\chi_1^-$ is prohibited and \tilde{b}_1 always decays to bottom quark and neutralinos. In the right of figure 6 we present the variations of the branching fraction as a function of the singlino/bino content of the LSP ($N_{1\tilde{S}/\tilde{B}}^2$) while the palette shows the simultaneously varying mass-splitting (Δm) between \tilde{b}_1 and the LSP.

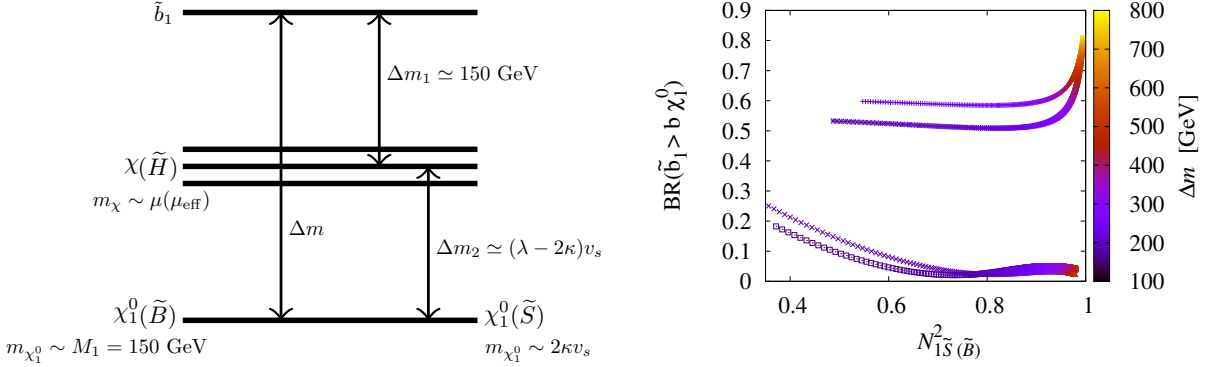


Figure 6. **Left:** Level diagram representing the spectrum comprising of a relatively light sbottom and a bino- (\tilde{B} ; in the MSSM) or a singlino-like (\tilde{S} ; in the NMSSM) LSP along with higgsino-like neutralinos and chargino sandwiched between them. **Right:** Variations of the effective branching fraction of a pair of sbottoms decaying into $2b\text{-jets} + \cancel{E}_T$ final state as a function of bino (singlino) content of the LSP, $N_{1\tilde{B}(\tilde{S})}^2$ in the MSSM (NMSSM). The upper (lower) pair of curves correspond to MSSM (NMSSM). In both cases $\mu/\mu_{\text{eff}} > 0 (< 0)$ is represented by the upper (lower) curve. The color palette indicates the simultaneously changing mass-splitting (Δm) between \tilde{b}_1 and the LSP. The following fixed values of various parameters are used: $\lambda = 0.7$, $\kappa = 0.18$ and $\tan\beta = 5$.

To conform to our broad scenario, we choose $\lambda = 0.7$ and $\kappa = 0.18$ with $\tan\beta = 5$ while $A_{\lambda,\kappa}$ are adjusted to obtain the mass of the SM-like Higgs boson in the right ballpark. Variations in both Δm and $N_{1\tilde{S}/\tilde{B}}^2$ are achieved by varying $|\mu_{\text{eff}}(\mu)|$ over the range 150-500 GeV. Note that in the NMSSM with $\mu_{\text{eff}} = \lambda v_S$ and $m_{\tilde{S}} \simeq 2\kappa v_S$, varying μ_{eff} results in a varying $m_{\tilde{S}}$ and hence in a changing LSP mass. At the same time, such a variation alters the splitting between the higgsino-like states and the LSP which is roughly given by $\Delta m_2 \approx (\lambda - 2\kappa)v_S$, as indicated in the level diagram of figure 6.

In the MSSM case we make a conservative choice of $M_1 = 150$ GeV for which any chargino mass is allowed [49]. Further, a minimum difference of 10 GeV between μ and M_1 is required with $|\mu| > M_1$. With this, the minimum bino fraction in the LSP that we could achieve in the MSSM is $\sim 50\%$ (which is manifested in the abrupt termination of the MSSM curves on the left side of the right plot of figure 6) when $|\mu| \simeq 160$ GeV. Note that for a similar higgsino content of the LSP the bino-higgsino mass difference in the MSSM is usually smaller than the singlino-higgsino mass difference in the NMSSM. Thus, with $m_{\tilde{b}_1} = 150 + \mu_{\text{eff}}(\mu)$, the decay

mode $\tilde{b}_1 \rightarrow b\chi_1^0$ gets more phase space in the NMSSM when compared to the MSSM case⁵.

The right plot of figure 6 shows that the effective branching fraction to the $2b + \cancel{E}_T$ final state (arising from \tilde{b}_1 pair production) can get severely suppressed in the NMSSM (with light singlino and higgsinos) when compared to an analogous neutralino spectrum in the MSSM (with light bino and higgsinos). This is so even though, as pointed out in the last paragraph, the available phase space is larger in the case of the NMSSM as compared to the MSSM. This suppression can clearly be attributed to the absence of any tree-level coupling of \tilde{b}_1 to a singlino-like LSP in the NMSSM as opposed to the presence of a tree-level coupling between the sbottom and the bino-like LSP in the MSSM. Furthermore, it is clear, as expected, that the NMSSM rates are decreasing with increasing singlino-content of the LSP. In the MSSM, because of similar couplings of $\tilde{b}_1 \equiv \tilde{b}_L$ to bino and the higgsinos (for our choice of $\tan\beta$), the branching ratio to the LSP is characteristically larger.⁶

Note that only L-type \tilde{b}_1 has been considered in figure 6. R-type \tilde{b}_1 with a larger hypercharge would always enhance the partial width for $\tilde{b}_1 \rightarrow b\chi_1^0$ in the MSSM with a bino-like LSP thus making the difference with NMSSM more drastic. Similarly, our generic choice of a smaller $\tan\beta$ would also lead to a smaller y_b thus suppressing the \tilde{b}_1 decays to higgsino-like states in the MSSM which would further favor its decay to the bino-like LSP in such a scenario.

5 Conclusions

In this work we discuss the characteristic phenomenology that the sbottoms could derive in a ‘natural’ NMSSM setup even though they do not actively address the issue of naturalness. We point out the generic possibility of having light sbottom(s) in such a scenario which could evade current bounds from the LHC experiments. The NMSSM setup considered in this work is characterized by relatively small μ_{eff} and light stop(s) which facilitate compliance with the standard notion of naturalness. The latter requires one to consider moderate to large values of λ in order to have the mass of the SM-like Higgs boson in the experimentally observed range.

It is stressed how the two ingredients that render the setup ‘natural’, i.e., small μ_{eff} ($|\mu_{\text{eff}}| \lesssim 350$ GeV) and large λ ($\sim 0.6 - 0.7$), could have an immediate impact on the sector

⁵Note, however, that with these choices the lightest sbottom might become as light as ~ 300 GeV which may still be allowed under certain circumstances [2]. In any case, given that the purpose here is to demonstrate how $\text{BR}[\tilde{b}_1 \rightarrow b \text{ LSP}]$ could get heavily suppressed for a singlino-like LSP, we choose not to get into the intricacies involving the possibility of such a light sbottom. Furthermore, in this discussion on variation of branching fraction, the more important parameter is the mass-splitting Δm (rather than the absolute mass of the LSP) and as long as it allows for a large enough \cancel{E}_T and render other final state objects visible, the discussion goes through.

⁶Further, note that this branching ratio does not initially vary appreciably as the bino fraction in the LSP increases since it is accompanied by a similar increase in the higgsino component of the NLSP neutralinos which are also kinematically accessible to $\tilde{b}_1 \equiv \tilde{b}_L$ to decay to. However, with increasing μ , in our setup, the mass-splitting between \tilde{b}_L and the LSP grows while the same with respect to the NLSPs remains roughly unaltered. Thus, the growing phase space explains the quick pick-up in $\text{BR}[\tilde{b}_1 \rightarrow b \text{ LSP}]$ at the right edge of the plot.

comprising of lighter neutralinos. While this combination tends to require a small v_S , large λ by itself implies small κ once absence of Landau pole below a high (unification) scale is demanded. These, in turn, drive the singlino mass ($= 2\kappa v_S$) small thus making it comparable or even smaller than μ_{eff} . Such a situation, in the presence of a large λ , could potentially make the lighter neutralino sector phenomenologically nontrivial. As far as the LSP is concerned, its composition could range between that like a nearly-pure singlino to a heavy mixture of singlino and higgsinos. This is accompanied by two neutralinos (immediately heavier than the LSP) whose compositions range between pure higgsinos and a similar mixture of higgsinos and singlino as in the case of the LSP. In the present context, this could crucially alter the ways in which sbottoms could decay. In our ‘simplified’ scenario we assume the soft gaugino masses, M_1 and M_2 (and M_3 as well) to be rather heavy. The lighter chargino is thus higgsino-like and the heavier electroweakinos and the gluino all decouple.

A further interesting observation in such an NMSSM framework (with large λ and light stops) pertains to the opening up of the rather low $\tan\beta$ ($\lesssim 2$) regime which is disfavored in the MSSM as it fails to find the mass of the SM-like Higgs boson in the right ballpark. A $\tan\beta$ value as low as 2 boosts the ratio $\frac{y_t}{y_b}$ thus quickly enhancing the y_t driven decays of \tilde{b}_1 over the y_b induced ones. This is found to be an important issue in the phenomenology of an L-type sbottom whose decay to higgsino-like chargino and a top quark is induced by y_t . Even more interestingly, the effect can be so strong that a 3-body decay of an L-type sbottom involving a y_t -driven vertex could overwhelm its y_b -induced 2-body decays to $b\chi_{1,2,3}^0$ for low to moderate virtuality of the propagating state (χ_1^\mp or the top quark). On the other hand, an enhanced $\frac{y_t}{y_b}$ could also ensure that a mostly R-type sbottom, with a tiny admixture of L-component, can have a significant branching fraction to $t\chi_1^-$.

We choose a few benchmark NMSSM scenarios satisfying the criteria mentioned above. These have the singlino-content of the LSP varying between 75% and 90%. The lighter sbottom can be (almost) purely R- or L-type. As pointed out in the last paragraph, we also discuss the interesting case of R-dominated lighter sbottom with a tiny admixture of the L-component. The mass of the lighter sbottom lies between 400 GeV and 600 GeV in these representative scenarios.

On the other hand, the heavier sbottom is arranged to be rather heavy ($\gtrsim 1.5$ TeV), in general. However, we showed (scenario BP4) that requiring even a small admixture of the L-component in an otherwise R-dominated light sbottom would result in a heavier sbottom not so different in mass from its lighter partner. Furthermore, scenarios with an L-type light sbottom inevitably have a stop squark in the spectrum of similar mass and hence should be simultaneously accessible at the LHC. In these two cases, a given final state may receive some limited contributions from more than one excitation (the heavier sbottom and the stop squarks) thus making its interpretation potentially involved. In the latter case, however, it is important to ensure that such a light sbottom indeed escapes the indirect bound that could be derived from non-observation of an accompanying light stop. Evading such a bound could be possible when the stop sector has an appreciable mixing and/or, for an unmixed L-type \tilde{t}_1 , if it could decay to heavier neutralinos. The former would, in turn, prompt the lighter stop to decay in multiple ways, with shared branching fractions.

For an L-type lighter sbottom, its $t\chi_1^-$ decay mode, if kinematically open, would dominate and would result in a healthy SSDL rate. A much enhanced SSDL rate might point to both sbottoms contributing to this final state with one of the sbottoms being L-type, for all practical purposes, while the mostly R-type one has a slight admixture of \tilde{b}_L . If $t\chi_1^-$ decay mode is not kinematically accessible, an L-type lighter sbottom would rather show up strongly in several multi-lepton final states. For a light NMSSM sbottom which is mostly R-type, the only resort to see its signature, in such a scenario, could be in the four-lepton final state.

The bottom line of the present study is that the signals of sbottoms in a natural NMSSM framework could be characteristically stubborn in not showing up promptly at the LHC experiments. This feature is crucially governed by the nature of the LSP. At the LHC Run-I this might have helped sbottoms escape the searches. On the other hand, the LHC-13 would require moderately large data (worth $\sim 300 \text{ fb}^{-1}$) to hint/establish their presence in various multi-lepton plus b -jets final states with \cancel{E}_T . There, it would be further corroborative if one experiences a dearth of events in the $2b$ -jets + \cancel{E}_T . Improved techniques proposed recently [70] could help sharpen the search for the sbottoms (and stops) in an involved situation. These observations should be helpful in planning future experimental analyses to uncover possible spectral configurations with light sbottoms and an LSP with a singlino-admixture in a ‘natural’ NMSSM setup.

Acknowledgments

JB and AC are partially supported by funding available from the Department of Atomic Energy, Government of India for the Regional Centre for Accelerator-based Particle Physics (RECAPP), Harish-Chandra Research Institute. AC acknowledges financial support from the Department of Science and Technology, Government of India through the INSPIRE Faculty Award /2016/DST/INSPIRE/04/2015/000110. The authors acknowledge the use of the cluster computing setup available at RECAPP and at the High Performance Computing facility of HRI. JB like to thank B. Fuks for very helpful discussions. The authors thank U. Chattopadhyay for his kind hospitality at the Theoretical Physics Group of the Indian Association for the Cultivation of Science, Kolkata where a part of the work is done. They also thank Amit Khulve and Ravindra Yadav for technical support.

References

- [1] CMS collaboration, V. Khachatryan et al., Searches for third-generation squark production in fully hadronic final states in proton-proton collisions at $\sqrt{s} = 8 \text{ TeV}$, *JHEP* **06** (2015) 116, [[1503.08037](#)].
- [2] ATLAS collaboration, G. Aad et al., ATLAS Run 1 searches for direct pair production of third-generation squarks at the Large Hadron Collider, *Eur. Phys. J.* **C75** (2015) 510, [[1506.08616](#)].
- [3] H. Li, W. Parker, Z. Si and S. Su, Sbottom Signature of the Supersymmetric Golden Region, *Eur. Phys. J.* **C71** (2011) 1584, [[1009.6042](#)].

- [4] A. Datta and S. Niyogi, Entangled System of Squarks from the Third Generation at the Large Hadron Collider, [1111.0200](#).
- [5] H. M. Lee, V. Sanz and M. Trott, Hitting sbottom in natural SUSY, *JHEP* **05** (2012) 139, [[1204.0802](#)].
- [6] E. Alvarez and Y. Bai, Reach the Bottom Line of the Sbottom Search, *JHEP* **08** (2012) 003, [[1204.5182](#)].
- [7] X.-J. Bi, Q.-S. Yan and P.-F. Yin, Light stop/sbottom pair production searches in the NMSSM, *Phys. Rev.* **D87** (2013) 035007, [[1209.2703](#)].
- [8] D. Ghosh and D. Sengupta, Searching the sbottom in the four lepton channel at the LHC, *Eur. Phys. J.* **C73** (2013) 2342, [[1209.4310](#)].
- [9] A. Chakraborty, D. K. Ghosh, D. Ghosh and D. Sengupta, Stop and sbottom search using dileptonic M_{T2} variable and boosted top technique at the LHC, *JHEP* **10** (2013) 122, [[1303.5776](#)].
- [10] G. Belanger, R. M. Godbole, S. Kraml and S. Kulkarni, Top Polarization in Sbottom Decays at the LHC, [1304.2987](#).
- [11] B. Batell, C. E. M. Wagner and L.-T. Wang, Constraints on a Very Light Sbottom, *JHEP* **05** (2014) 002, [[1312.2590](#)].
- [12] P. Huang and C. E. M. Wagner, CMS kinematic edge from sbottoms, *Phys. Rev.* **D91** (2015) 015014, [[1410.4998](#)].
- [13] A. Kobakhidze, N. Liu, L. Wu and J. M. Yang, ATLAS Z-peaked excess in the MSSM with a light sbottom or stop, *Phys. Rev.* **D92** (2015) 075008, [[1504.04390](#)].
- [14] B. Dutta, A. Gurrola, K. Hatakeyama, W. Johns, T. Kamon, P. Sheldon et al., Probing Compressed Bottom Squarks with Boosted Jets and Shape Analysis, *Phys. Rev.* **D92** (2015) 095009, [[1507.01001](#)].
- [15] T. Han, S. Su, Y. Wu, B. Zhang and H. Zhang, Sbottom discovery via mixed decays at the LHC, *Phys. Rev.* **D92** (2015) 115009, [[1507.04006](#)].
- [16] R. Barbieri and G. F. Giudice, Upper Bounds on Supersymmetric Particle Masses, *Nucl. Phys.* **B306** (1988) 63.
- [17] T. Cheng, J. Li, T. Li and Q.-S. Yan, Natural NMSSM confronting with the LHC7-8, *Phys. Rev.* **D89** (2014) 015015, [[1304.3182](#)].
- [18] C. Han, K.-i. Hikasa, L. Wu, J. M. Yang and Y. Zhang, Current experimental bounds on stop mass in natural SUSY, *JHEP* **10** (2013) 216, [[1308.5307](#)].
- [19] S. Zheng and Y. Yu, Constraints on Natural Supersymmetry from Electroweak Precision Tests, *JHEP* **01** (2015) 106, [[1405.6446](#)].
- [20] P. Grothaus, S. P. Liew and K. Sakurai, A closer look at a hint of SUSY at the 8 TeV LHC, *JHEP* **05** (2015) 133, [[1502.05712](#)].
- [21] M. E. Peskin and T. Takeuchi, A New constraint on a strongly interacting Higgs sector, *Phys. Rev. Lett.* **65** (1990) 964–967.
- [22] H. Baer, V. Barger, P. Huang, A. Mustafayev and X. Tata, Radiative natural SUSY with a 125 GeV Higgs boson, *Phys. Rev. Lett.* **109** (2012) 161802, [[1207.3343](#)].

- [23] H. Baer, V. Barger, P. Huang, D. Mickelson, A. Mustafayev and X. Tata, Naturalness, Supersymmetry and Light Higgsinos: A Snowmass Whitepaper, in Community Summer Study 2013: Snowmass on the Mississippi (CSS2013) Minneapolis, MN, USA, July 29-August 6, 2013, 2013. [1306.2926](#).
- [24] A. Mustafayev and X. Tata, Supersymmetry, Naturalness, and Light Higgsinos, [Indian J. Phys. **88** \(2014\) 991–1004](#), [[1404.1386](#)].
- [25] H. Baer, V. Barger and M. Savoy, Upper bounds on sparticle masses from naturalness or how to disprove weak scale supersymmetry, [Phys. Rev. **D93** \(2016\) 035016](#), [[1509.02929](#)].
- [26] CMS collaboration, S. Chatrchyan et al., Search for new physics in events with same-sign dileptons and jets in pp collisions at $\sqrt{s} = 8$ TeV, [JHEP **01** \(2014\) 163](#), [[1311.6736](#)].
- [27] ATLAS collaboration, G. Aad et al., Search for direct top-squark pair production in final states with two leptons in pp collisions at $\sqrt{s} = 8$ TeV with the ATLAS detector, [JHEP **06** \(2014\) 124](#), [[1403.4853](#)].
- [28] ATLAS collaboration, G. Aad et al., Search for supersymmetry at $\sqrt{s}=8$ TeV in final states with jets and two same-sign leptons or three leptons with the ATLAS detector, [JHEP **06** \(2014\) 035](#), [[1404.2500](#)].
- [29] U. Ellwanger, C. Hugonie and A. M. Teixeira, The Next-to-Minimal Supersymmetric Standard Model, [Phys. Rept. **496** \(2010\) 1–77](#), [[0910.1785](#)].
- [30] Y. Bai, H.-C. Cheng, J. Gallicchio and J. Gu, Stop the Top Background of the Stop Search, [JHEP **07** \(2012\) 110](#), [[1203.4813](#)].
- [31] J. Beuria, A. Chatterjee, A. Datta and S. K. Rai, Two Light Stops in the NMSSM and the LHC, [JHEP **09** \(2015\) 073](#), [[1505.00604](#)].
- [32] J. S. Kim, D. Schmeier and J. Tattersall, Role of the ‘N’ in the natural NMSSM for the LHC, [Phys. Rev. **D93** \(2016\) 055018](#), [[1510.04871](#)].
- [33] U. Ellwanger, G. Espitalier-Noel and C. Hugonie, Naturalness and Fine Tuning in the NMSSM: Implications of Early LHC Results, [JHEP **09** \(2011\) 105](#), [[1107.2472](#)].
- [34] D. Das, U. Ellwanger and A. M. Teixeira, Modified Signals for Supersymmetry in the NMSSM with a Singlino-like LSP, [JHEP **04** \(2012\) 067](#), [[1202.5244](#)].
- [35] U. Ellwanger, Testing the higgsino-singlino sector of the NMSSM with trileptons at the LHC, [JHEP **11** \(2013\) 108](#), [[1309.1665](#)].
- [36] J. S. Kim and T. S. Ray, The higgsino-singlino world at the large hadron collider, [Eur. Phys. J. **C75** \(2015\) 40](#), [[1405.3700](#)].
- [37] U. Ellwanger and A. M. Teixeira, NMSSM with a singlino LSP: possible challenges for searches for supersymmetry at the LHC, [JHEP **10** \(2014\) 113](#), [[1406.7221](#)].
- [38] J. Cao, L. Shang, P. Wu, J. M. Yang and Y. Zhang, Supersymmetry explanation of the Fermi Galactic Center excess and its test at LHC run II, [Phys. Rev. **D91** \(2015\) 055005](#), [[1410.3239](#)].
- [39] C. T. Potter, Natural NMSSM with a Light Singlet Higgs and Singlino LSP, [Eur. Phys. J. **C76** \(2016\) 44](#), [[1505.05554](#)].
- [40] U. Ellwanger, Higgs Bosons in the Next-to-Minimal Supersymmetric Standard Model at the LHC, [Eur. Phys. J. **C71** \(2011\) 1782](#), [[1108.0157](#)].

- [41] S. F. King, M. Muhlleitner and R. Nevzorov, NMSSM Higgs Benchmarks Near 125 GeV, *Nucl. Phys.* **B860** (2012) 207–244, [[1201.2671](#)].
- [42] S. F. King, M. Mühlleitner, R. Nevzorov and K. Walz, Natural NMSSM Higgs Bosons, *Nucl. Phys.* **B870** (2013) 323–352, [[1211.5074](#)].
- [43] S. Kraml and W. Porod, Sfermion decays into singlets and singlinos in the NMSSM, *Phys. Lett.* **B626** (2005) 175–183, [[hep-ph/0507055](#)].
- [44] A. Bartl, S. Hesselbach, K. Hidaka, T. Kernreiter and W. Porod, Top squarks and bottom squarks in the MSSM with complex parameters, *Phys. Rev.* **D70** (2004) 035003, [[hep-ph/0311338](#)].
- [45] S. Y. Choi, D. J. Miller and P. M. Zerwas, The Neutralino sector of the next-to-minimal supersymmetric standard model, *Nucl. Phys.* **B711** (2005) 83–111, [[hep-ph/0407209](#)].
- [46] ATLAS collaboration, G. Aad et al., Search for supersymmetry at $\sqrt{s} = 13$ TeV in final states with jets and two same-sign leptons or three leptons with the ATLAS detector, [1602.09058](#).
- [47] M. Drees, H. Dreiner, D. Schmeier, J. Tattersall and J. S. Kim, CheckMATE: Confronting your Favourite New Physics Model with LHC Data, *Comput. Phys. Commun.* **187** (2014) 227–265, [[1312.2591](#)].
- [48] J. S. Kim, D. Schmeier, J. Tattersall and K. Rolbiecki, A framework to create customised LHC analyses within CheckMATE, *Comput. Phys. Commun.* **196** (2015) 535–562, [[1503.01123](#)].
- [49] ATLAS collaboration, G. Aad et al., Search for the electroweak production of supersymmetric particles in $\sqrt{s}=8$ TeV pp collisions with the ATLAS detector, *Phys. Rev.* **D93** (2016) 052002, [[1509.07152](#)].
- [50] CMS collaboration, V. Khachatryan et al., Searches for electroweak production of charginos, neutralinos, and sleptons decaying to leptons and W, Z, and Higgs bosons in pp collisions at 8 TeV, *Eur. Phys. J.* **C74** (2014) 3036, [[1405.7570](#)].
- [51] Q.-F. Xiang, X.-J. Bi, P.-F. Yin and Z.-H. Yu, Searching for Singlino-Higgsino Dark Matter in the NMSSM, [1606.02149](#).
- [52] U. Ellwanger, J. F. Gunion and C. Hugonie, NMHDECAY: A Fortran code for the Higgs masses, couplings and decay widths in the NMSSM, *JHEP* **02** (2005) 066, [[hep-ph/0406215](#)].
- [53] U. Ellwanger and C. Hugonie, NMHDECAY 2.0: An Updated program for sparticle masses, Higgs masses, couplings and decay widths in the NMSSM, *Comput. Phys. Commun.* **175** (2006) 290–303, [[hep-ph/0508022](#)].
- [54] U. Ellwanger and C. Hugonie, NMSPEC: A Fortran code for the sparticle and Higgs masses in the NMSSM with GUT scale boundary conditions, *Comput. Phys. Commun.* **177** (2007) 399–407, [[hep-ph/0612134](#)].
- [55] D. Das, U. Ellwanger and A. M. Teixeira, NMSDECAY: A Fortran Code for Supersymmetric Particle Decays in the Next-to-Minimal Supersymmetric Standard Model, *Comput. Phys. Commun.* **183** (2012) 774–779, [[1106.5633](#)].
- [56] M. Muhlleitner, A. Djouadi and Y. Mambrini, SDECAY: A Fortran code for the decays of the supersymmetric particles in the MSSM, *Comput. Phys. Commun.* **168** (2005) 46–70, [[hep-ph/0311167](#)].

- [57] J. Alwall, R. Frederix, S. Frixione, V. Hirschi, F. Maltoni, O. Mattelaer et al., The automated computation of tree-level and next-to-leading order differential cross sections, and their matching to parton shower simulations, *JHEP* **07** (2014) 079, [[1405.0301](#)].
- [58] NNPDF collaboration, R. D. Ball et al., Parton distributions for the LHC Run II, *JHEP* **04** (2015) 040, [[1410.8849](#)].
- [59] W. Beenakker, R. Hopker and M. Spira, PROSPINO: A Program for the production of supersymmetric particles in next-to-leading order QCD, [hep-ph/9611232](#).
- [60] T. Sjöstrand, S. Ask, J. R. Christiansen, R. Corke, N. Desai, P. Ilten et al., An Introduction to PYTHIA 8.2, *Comput. Phys. Commun.* **191** (2015) 159–177, [[1410.3012](#)].
- [61] T. Sjostrand, S. Mrenna and P. Z. Skands, PYTHIA 6.4 Physics and Manual, *JHEP* **05** (2006) 026, [[hep-ph/0603175](#)].
- [62] M. L. Mangano, M. Moretti, F. Piccinini and M. Treccani, Matching matrix elements and shower evolution for top-quark production in hadronic collisions, *JHEP* **01** (2007) 013, [[hep-ph/0611129](#)].
- [63] J. Alwall et al., Comparative study of various algorithms for the merging of parton showers and matrix elements in hadronic collisions, *Eur. Phys. J.* **C53** (2008) 473–500, [[0706.2569](#)].
- [64] M. Selvaggi, DELPHES 3: A modular framework for fast-simulation of generic collider experiments, *J. Phys. Conf. Ser.* **523** (2014) 012033.
- [65] M. Cacciari, G. P. Salam and G. Soyez, FastJet User Manual, *Eur. Phys. J.* **C72** (2012) 1896, [[1111.6097](#)].
- [66] E. Conte, B. Fuks and G. Serret, MadAnalysis 5, A User-Friendly Framework for Collider Phenomenology, *Comput. Phys. Commun.* **184** (2013) 222–256, [[1206.1599](#)].
- [67] E. Conte, B. Dumont, B. Fuks and C. Wymant, Designing and recasting LHC analyses with MadAnalysis 5, *Eur. Phys. J.* **C74** (2014) 3103, [[1405.3982](#)].
- [68] B. Dumont, B. Fuks, S. Kraml, S. Bein, G. Chalons, E. Conte et al., Toward a public analysis database for LHC new physics searches using MADANALYSIS 5, *Eur. Phys. J.* **C75** (2015) 56, [[1407.3278](#)].
- [69] H.-C. Cheng and Z. Han, Minimal Kinematic Constraints and $m(T2)$, *JHEP* **12** (2008) 063, [[0810.5178](#)].
- [70] M. Schlaffer, M. Spannowsky and A. Weiler, Searching for supersymmetry scalelessly, [1603.01638](#).